Segmentation of Structures for Improved Thermal Stability and Mechanical Interchangeability

John Hart (ajhart@mit.edu)
B.S.E. Mechanical Engineering, University of Michigan (April 2000)
S.M. Mechanical Engineering, MIT (February 2002)
January 30, 2002

Thesis Advisor: Prof. Alexander Slocum
MIT Precision Engineering Research Group

Overview

PROBLEM: Structural design and component packaging of conventional microscopes makes them inadequate for nanoscale observations.

Specifically, need improvements in:

1. Stability.
2. Flexibility.
3. Resolution.

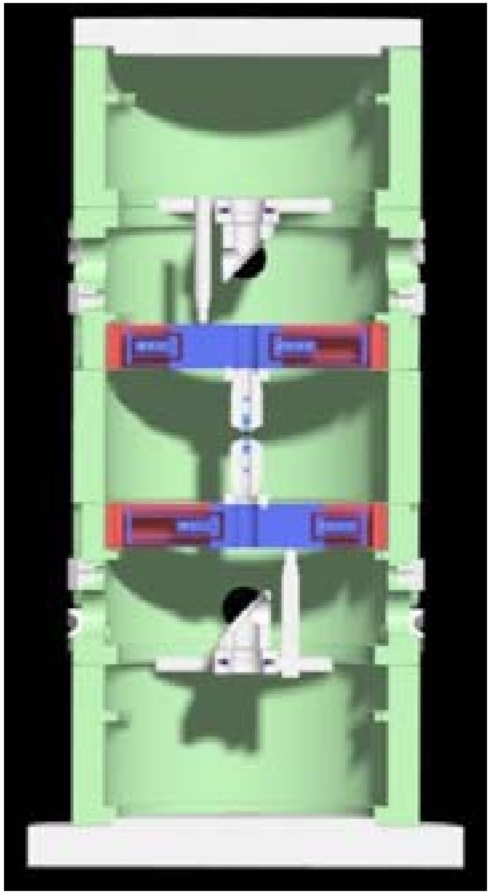

SOLUTION: A symmetric, segmented structure:

- Tubular modules encourage uniform thermal expansion.
- Kinematic couplings between modules enable reassembly and reconfiguration with sub-micron repeatability.

HPM Project

The High Precision Microscope (HPM) Project seeks a new microscope for advanced biological experiments [1]:

- First use examining DNA strands during protein binding.
- Goal to improve:
  - Thermal stability.
  - Reconfigurability.
  - Design of optics, positioning actuators, and positioning stages.

Work at MIT PERG during the past year to:

1. Design the HPM structure.
2. Test the structure's thermal stability and optimize through FEA.
3. Model kinematic coupling interchangeability.

Conventional Microscope Design

Designed for manual, one-sided examinations:

- Asymmetry of structures causes thermal tilt errors.
- Must be inverted and stacked for two-sided experiments.
- Difficult to switch optics, stages, etc.

1900

2000

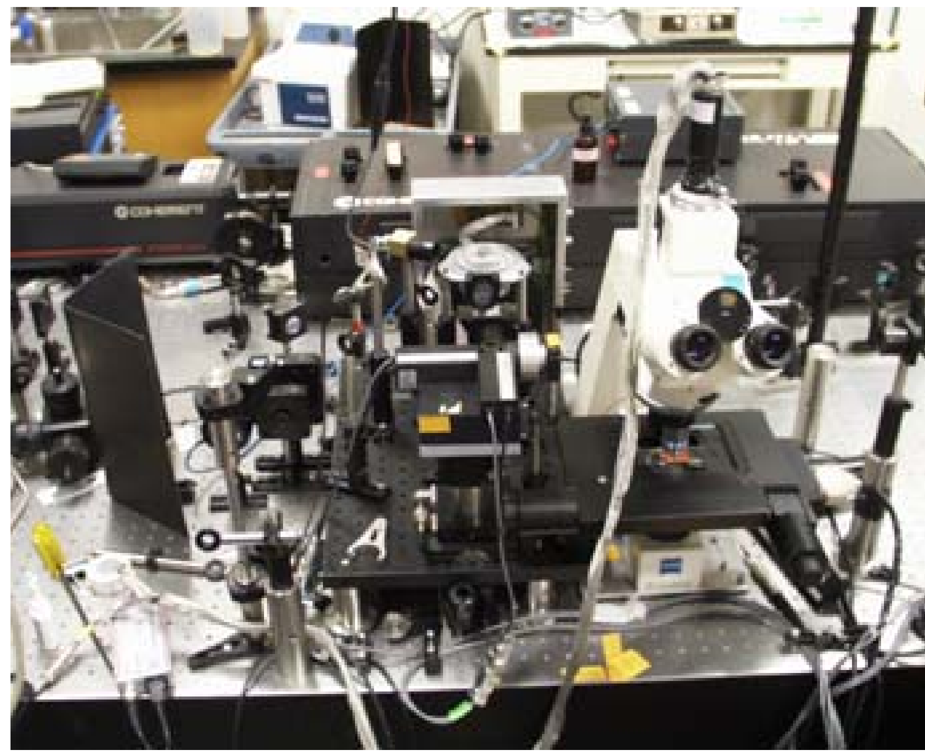

Functional Requirements

1. Minimize structural sensitivity to thermal drift.
2. Support multiple optical paths.
3. Enable optics modules to be interchanged without recalibration.
4. Maintain stiffness close to that of a monolithic structure.

→ In the future, accommodate:

- Picomotor/flexure drives for the optics.
- Multi-axis flexure stage for sample.

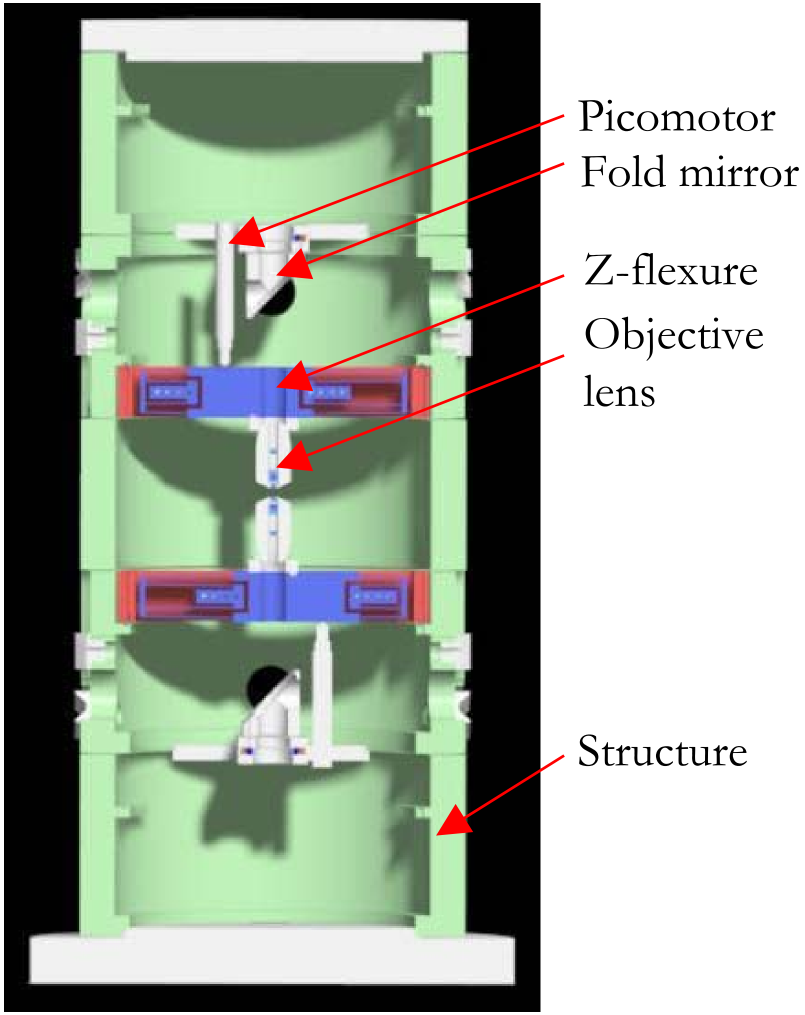

Segmented Structure Design

A modular tubular structure with kinematic couplings as interconnects*:

- Gaps constrain axial heat flow and relieve thermal stresses.
- Heat flows more circumferentially, making axial expansion of the stack more uniform.
- Canoe ball kinematic couplings give:
  - Little contact, high-stiffness.
  - Sliding freedom for uniform radial tube expansion.
  - Sub-micron repeatability for interchanging modules.

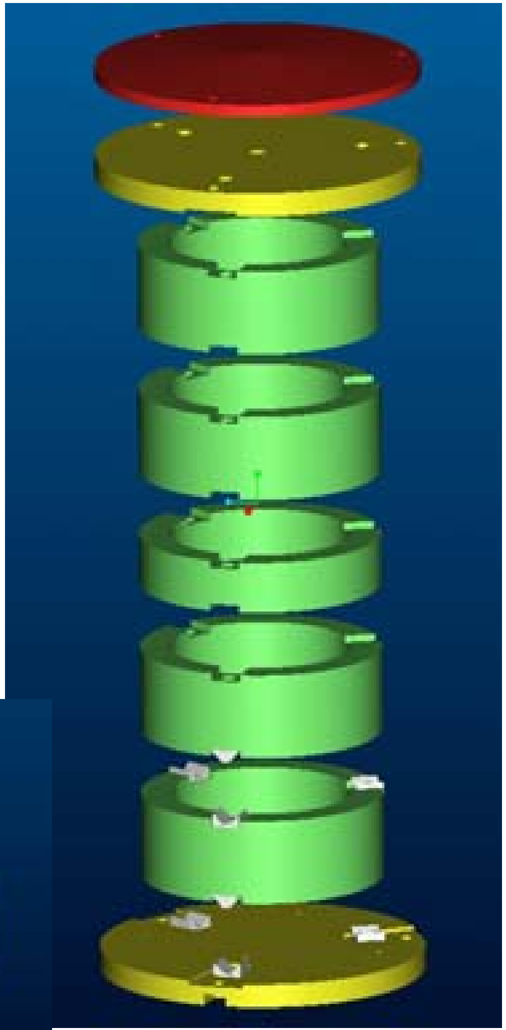

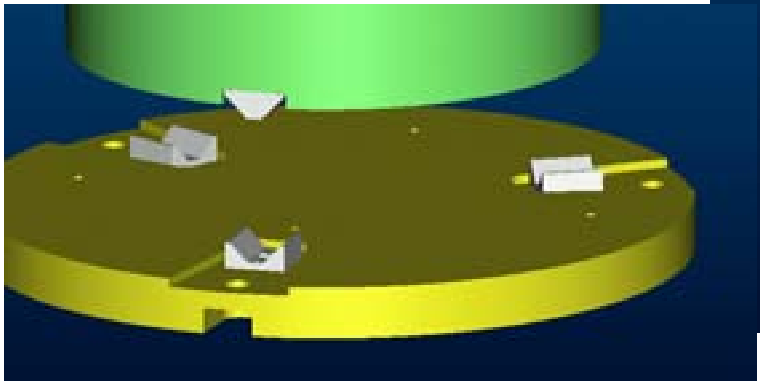

*Collaboration with Matt Sweetland

Heat Flow Theory

Locally apply heat to the midpoint of one side of a hollow tube:

- **Larger tube:**
  - Circular isotherms.
  - Uniform radial heat flow.
- **Shorter tube = axial constraint:**
  - Isotherms pushed circumferentially.
  - Gaps have negligible contact, high resistance.

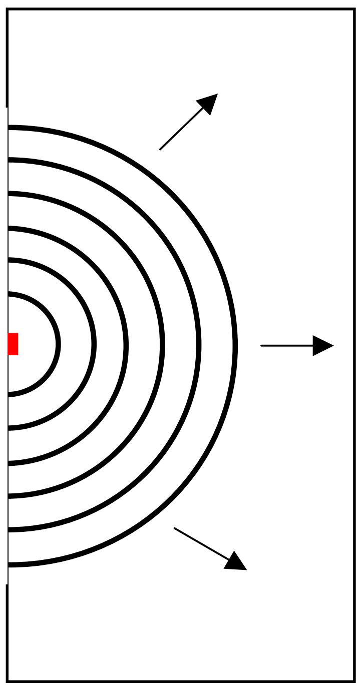

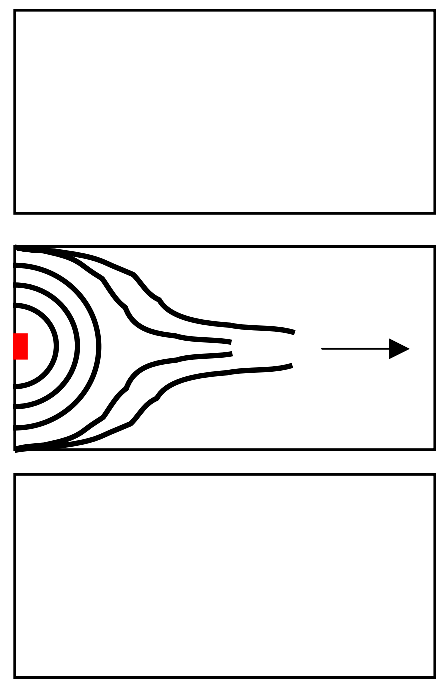

Thermal Expansion Theory

Circumferential temperature difference causes asymmetric axial growth [2]:

$$\delta = \alpha_t L_o \left(\overline{T_h} - \overline{T_n} \right) = \alpha_t \int_0^{L_o} \left(T_h(z) - T_n(z) \right) dz$$

$$\theta_{tilt} = \tan^{-1}\left(\frac{\delta}{D_0} \right)$$

$$\rightarrow \quad \delta_{obj} = L_s \frac{\alpha_t L_o \left(\overline{T_h} - \overline{T_n} \right)}{D_o}$$

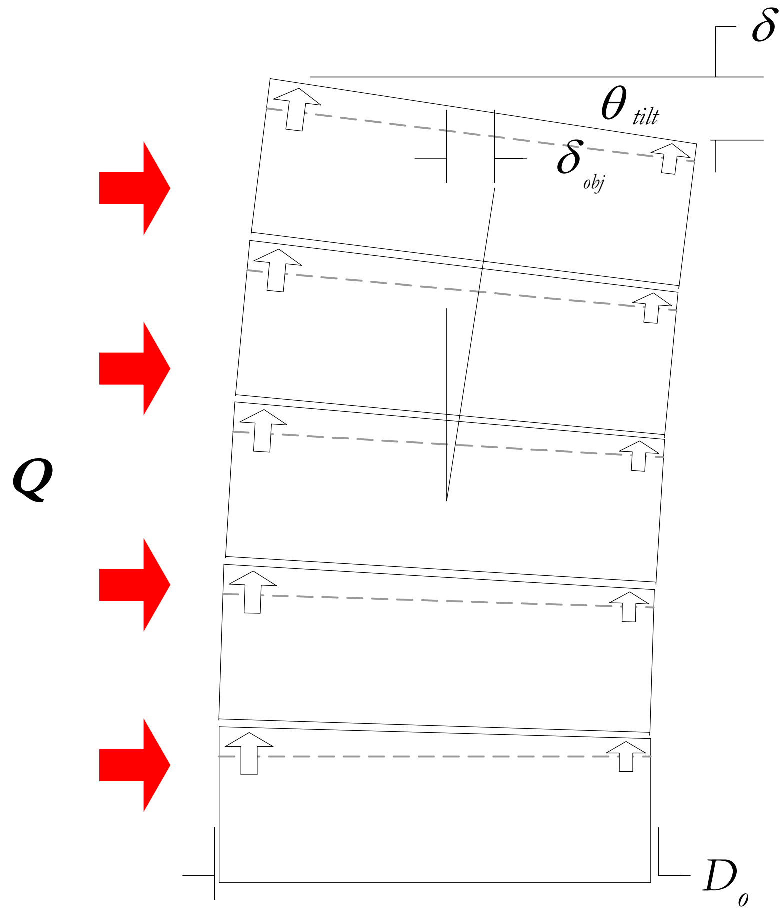

Steady-State Expansion Model

- Assume axially uniform temperature on each segment:

$$\delta_{obj} = \alpha_t \left[\left(\sum_{i=1}^{5} L_i T_i \right)_{heated} - \left(\sum_{i=1}^{5} L_i T_i \right)_{nheated} \right]$$

- Material performance indices:

$$G_{ss} = \left(\frac{k}{\alpha_t} \right) \qquad G_{tr} = \left(\frac{\alpha}{\alpha_t} \right)$$

k = Thermal conductivity
α = Thermal diffusivity
α_t = Coefficient of thermal expansion

Measurement Points:

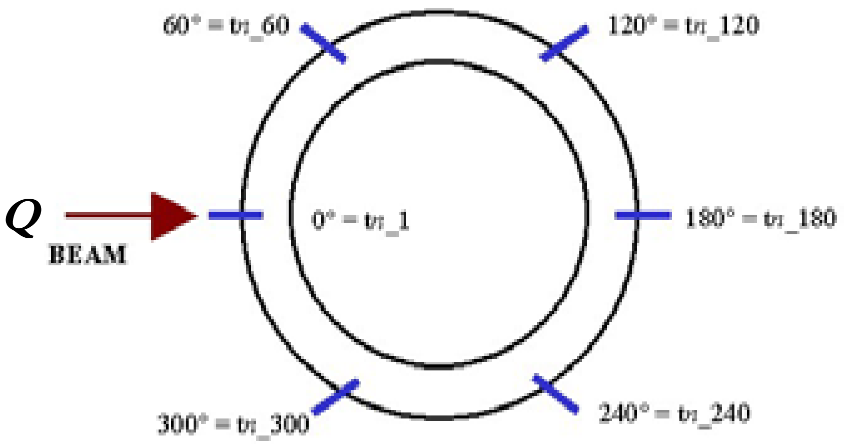

Transient Expansion Model

- Slice each segment, model as semi-infinite bodies [3], and project the axial heat flow:

$$T_{norm} = \frac{T(x,t) - T(t=0)}{\overline{T_{s,n}} - T(t=0)} = 1 - \operatorname{erf}\left(\frac{z}{2\sqrt{\alpha t}}\right)$$

- Moving average update of midpoint temperature of each slice [4]:

$$\overline{T_{s,n}} = \left(\frac{n-1}{n}\right)\overline{T_{s,n-1}} + \frac{T_{s,n}}{n}$$

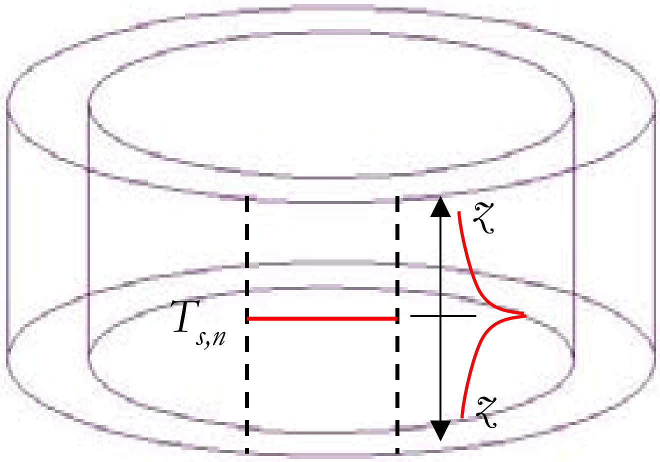

→ **Approaches a crude finite element method in 2D (*z*, θ) + time.**

Finite Element Models

Sequential thermal and structural simulations (Pro/MECHANICA):

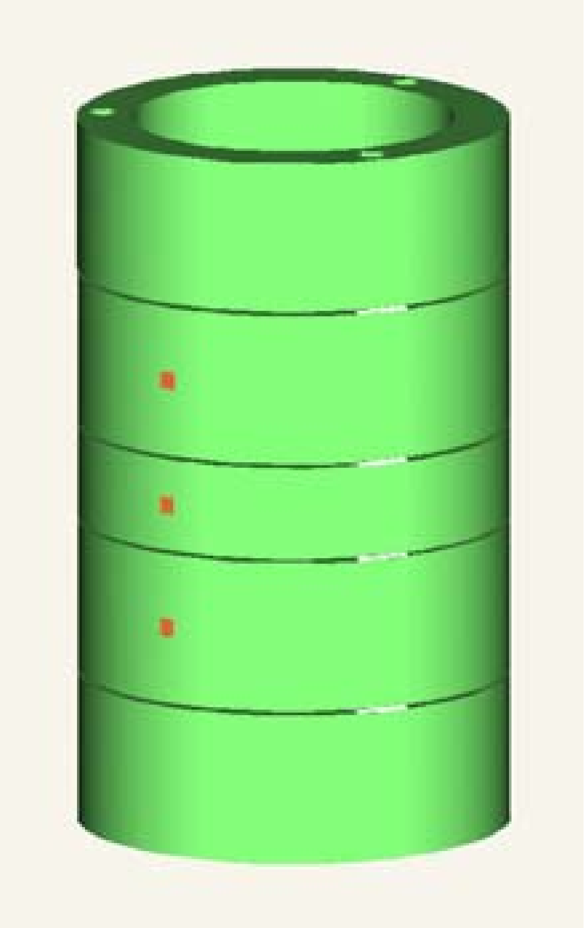

Thermal
- Couplings as 1” x 1” patches.
- Three 1W ½” x ½” heat sources.
- Uniform free convection loss on outside, *h* = 1.96.

→ Solved for steady-state temperature distribution.

Structural
- Specify steady-state temperatures as boundary condition.
- Constrain non-sliding DOF at bottom couplings.

→ Solved for steady-state deflections.

Simulated Isotherms

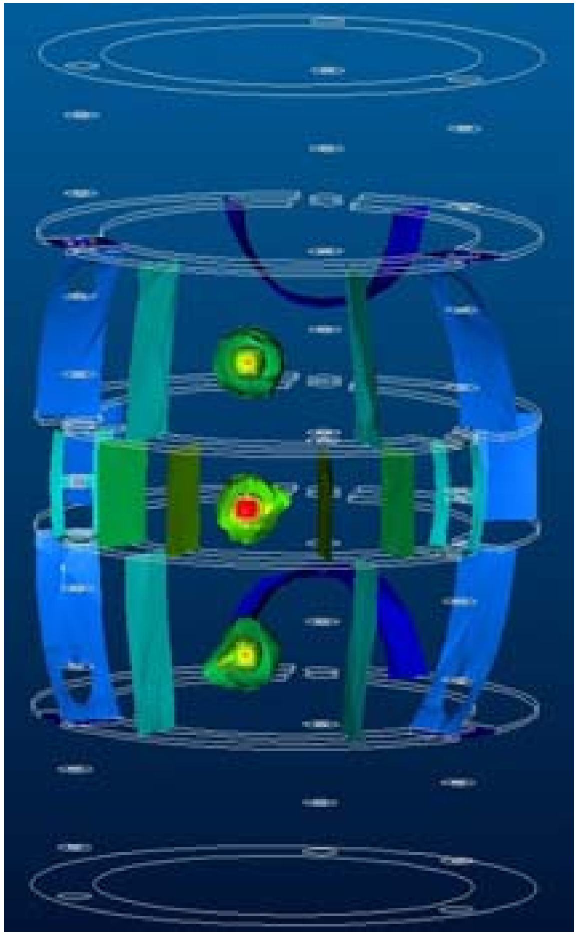

Segmented

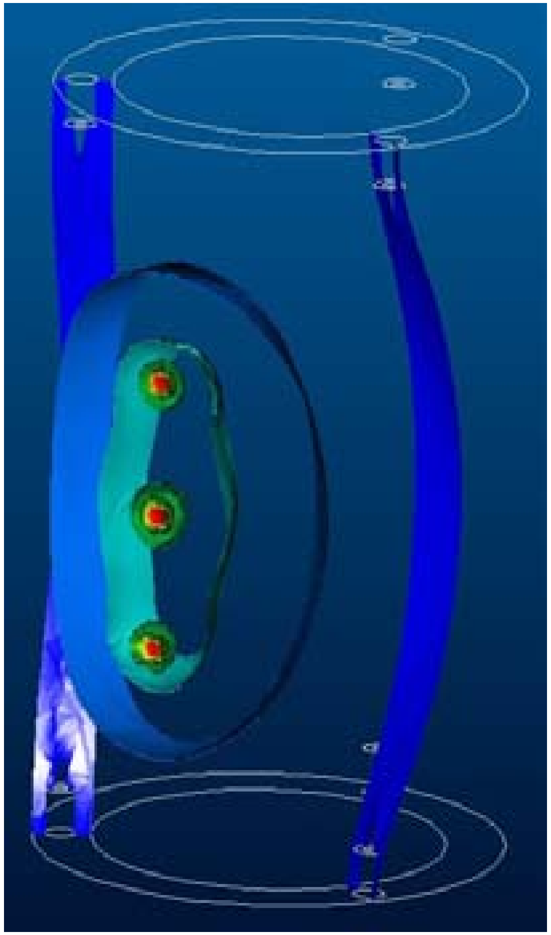

One-Piece

Resonant Behavior

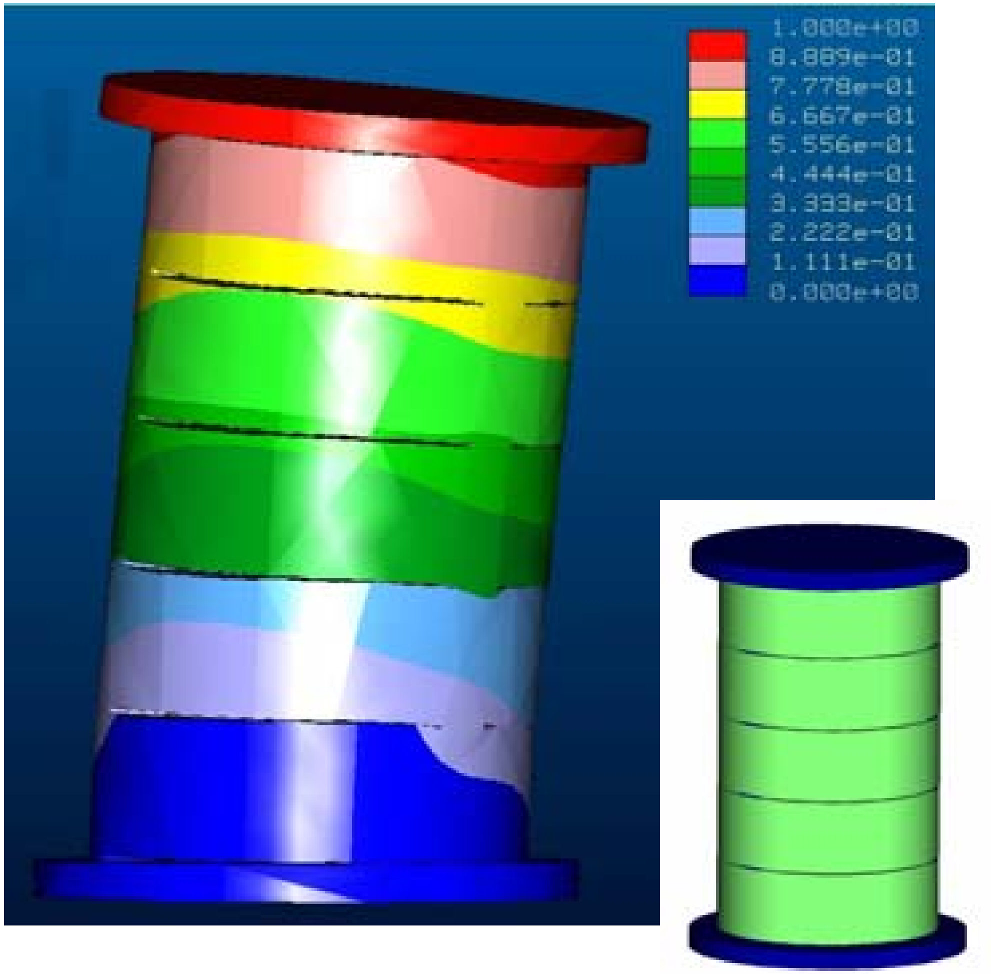

Segmented: $\omega_{n,1}$ = 356 Hz

One-Piece: $\omega_{n,1}$ = 253 Hz

<u>29% Reduction</u>

Experiments

Measured tilt under controlled boundary conditions for 8-hour durations*:

- Tube structure mounted between two plates and preloaded with threaded rods.
- Isolated from vibration on optics table.
- Isolated from thermal air currents using 4”-wall thickness foam chamber.
- 54 3-wire platinum RTD’s; 0.008° C (16-bit) resolution; +/- 1.5° C relative accuracy.
- Tilt measured using Zygo differential plane mirror interferometer (DPMI); 0.06 arcsec resolution = 72 nm drift of the objective.
- Three 1W disturbances to stack side by direct contact of copper thin-film sources.

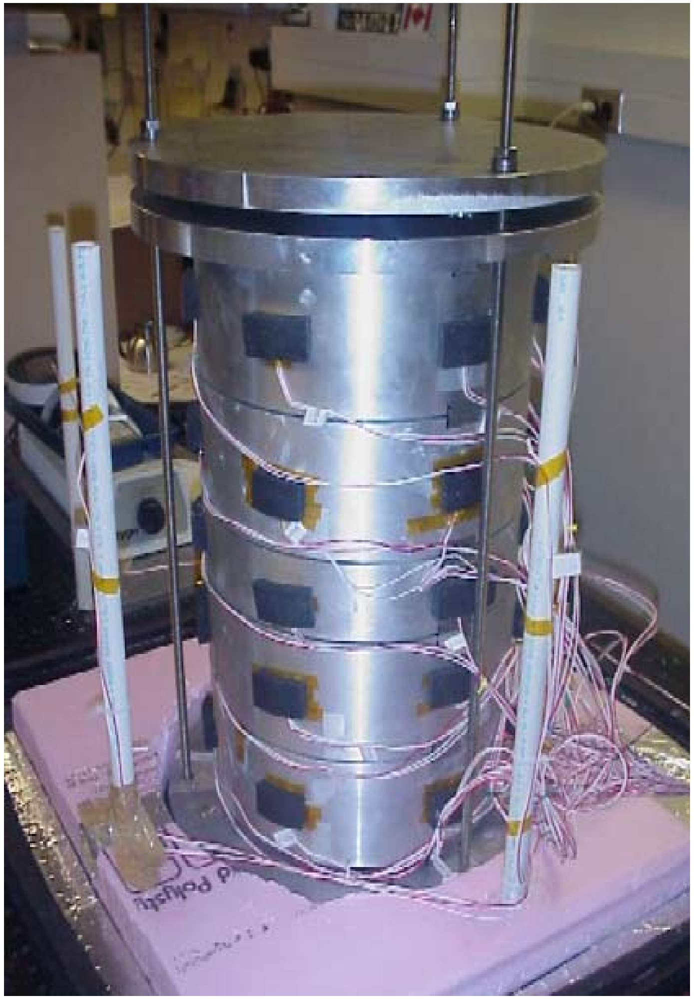

*Fabrication and measurement help from Philip Loiselle.

Experiments

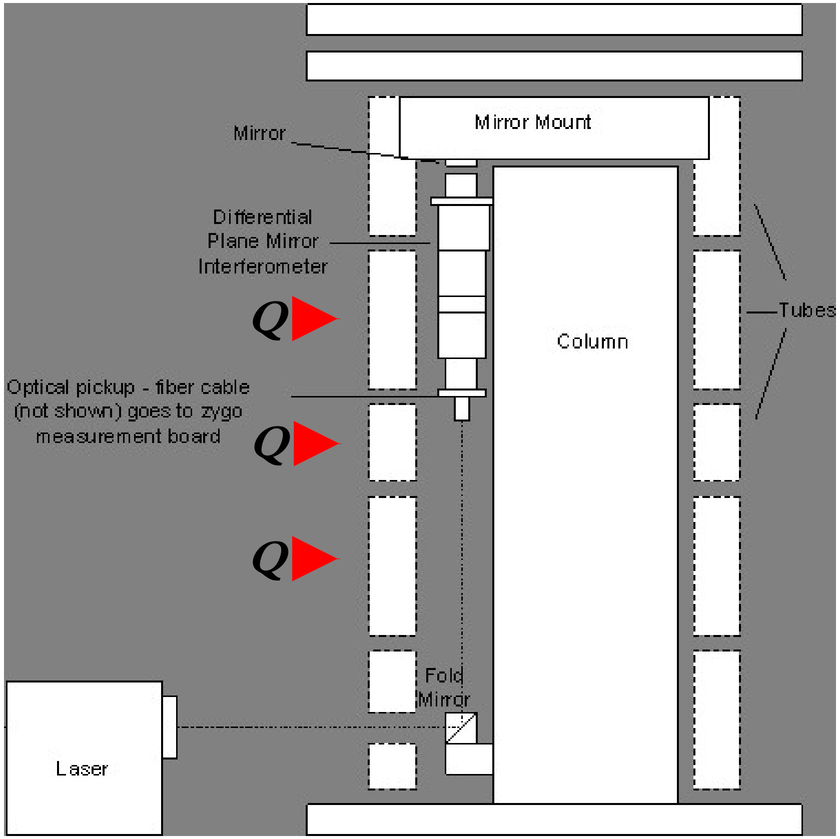

Tilt Error - Experimental

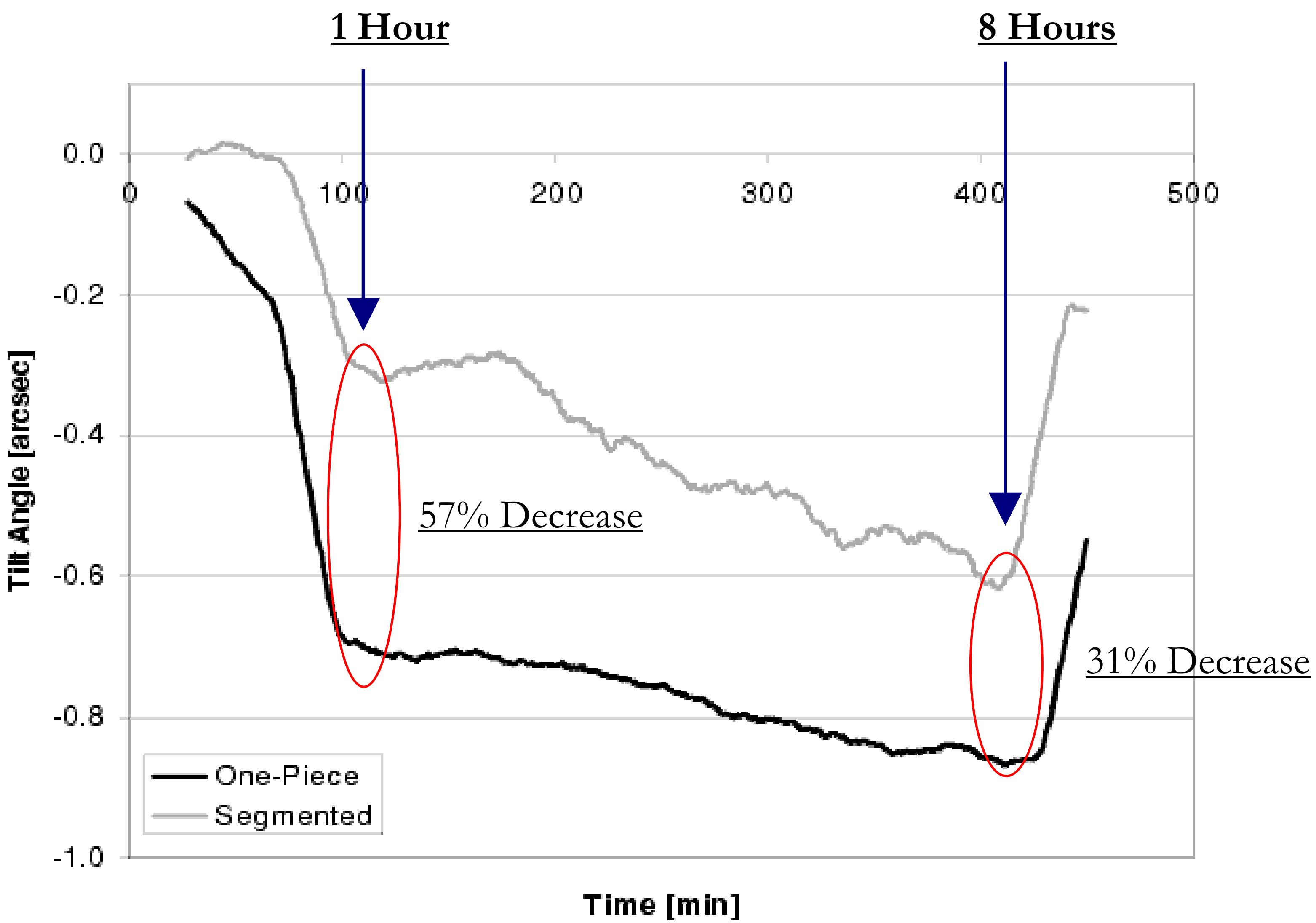

Circumferential Heat Flow

Heated segment:

- Near-perfect bulk heating after decay of ~20 minute transient
- ~1.60° C total increase.

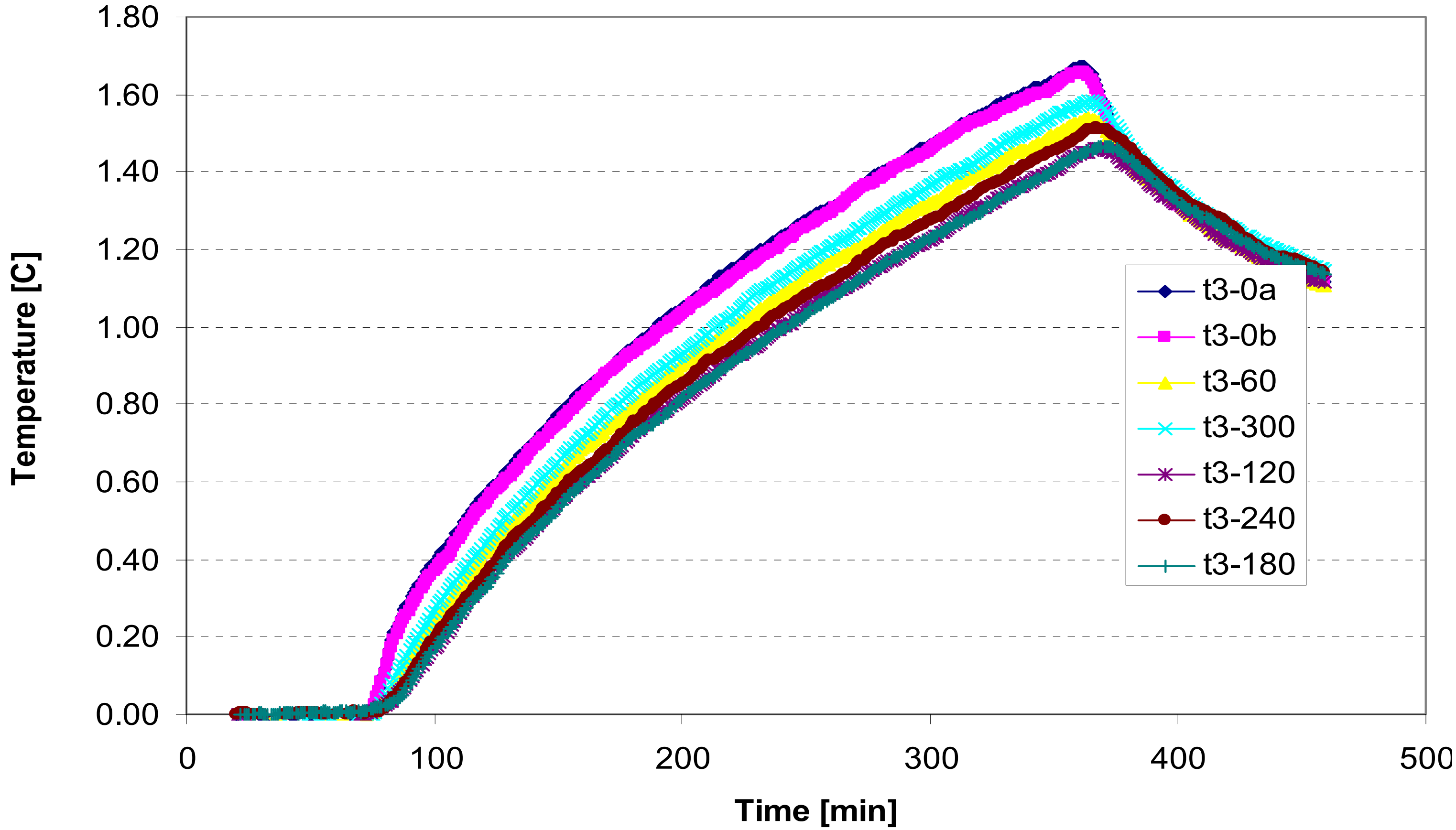

Circumferential Heat Flow

Non-heated segment:

- Near-perfect bulk heating.
- ~1.0° C total increase.

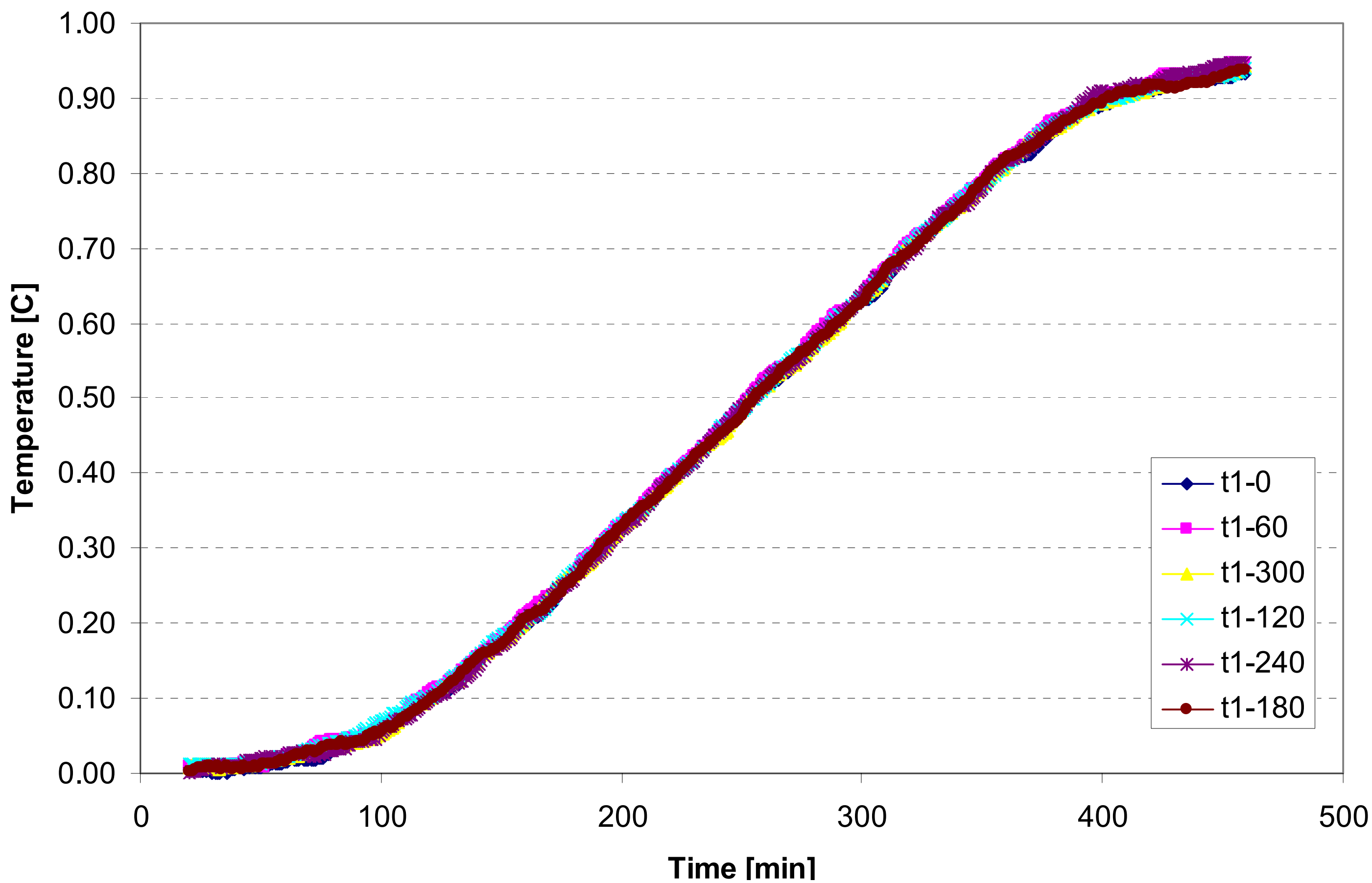

Circumferential Heat Flow

Center segment: difference between heated and opposite (180°) points:

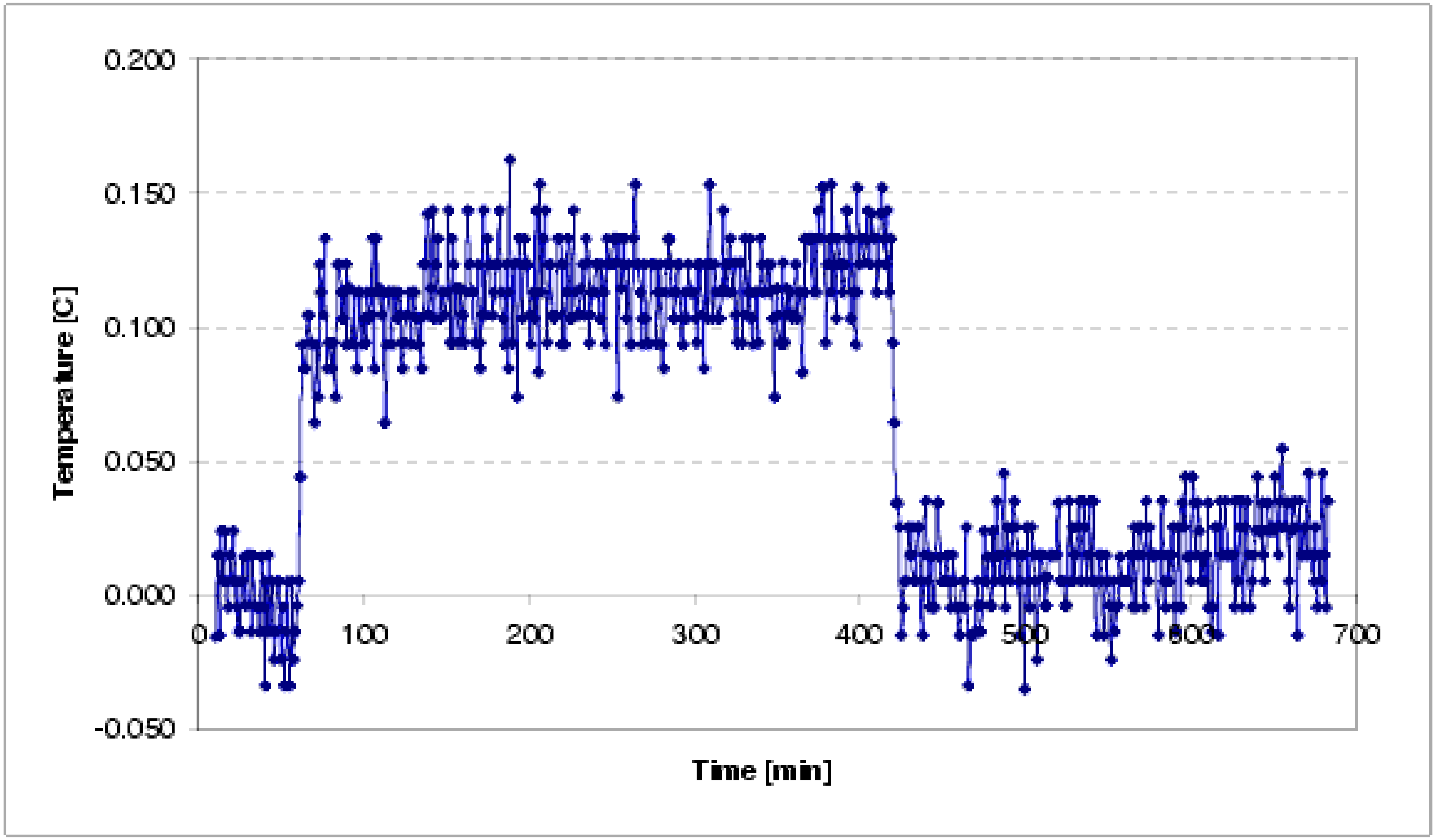

Analytical Models vs. Experiments

- Steady-state prediction is correct for final value.
- Transient prediction fits for first hour; diverges afterward.

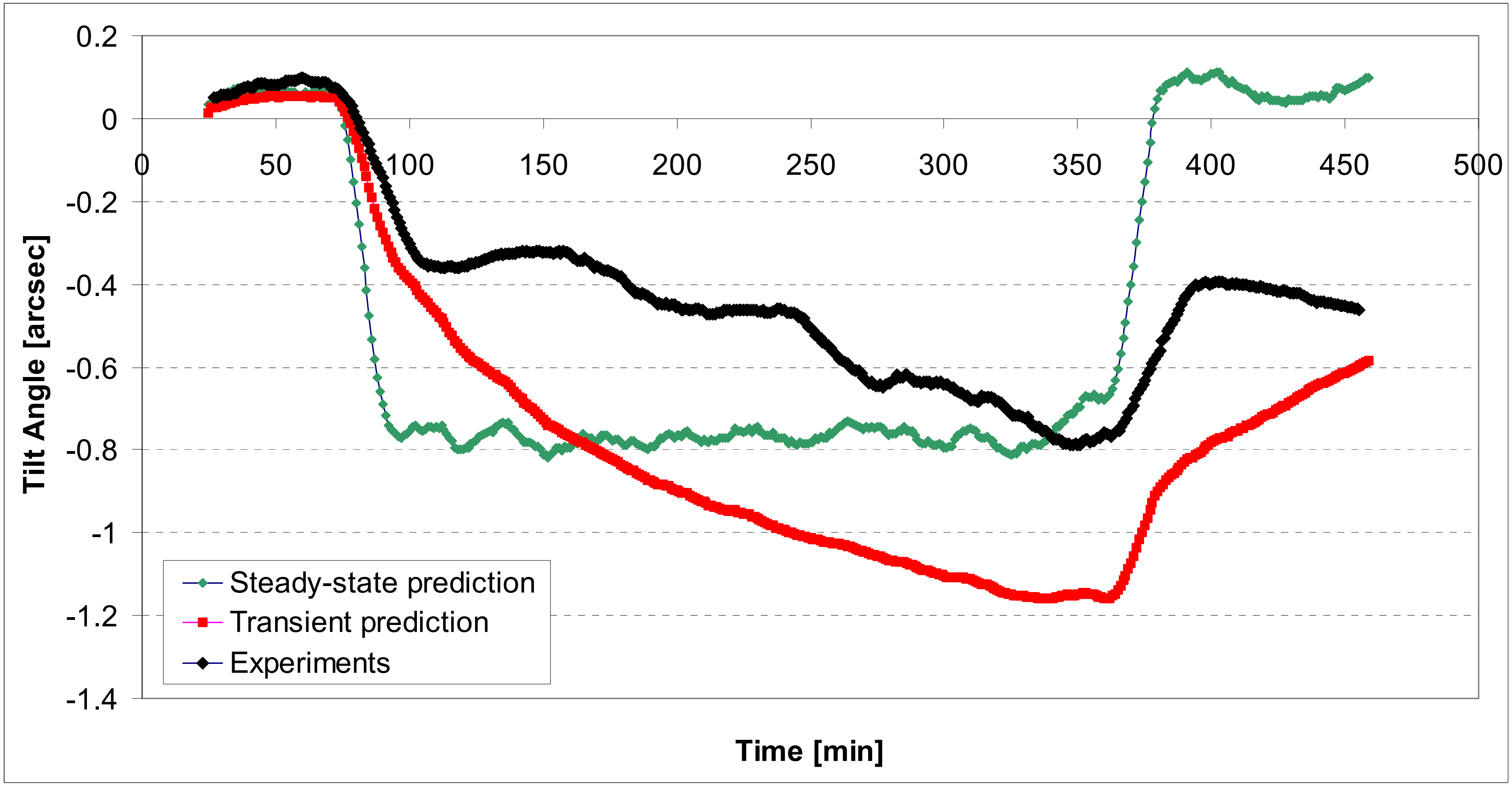

FEA vs. Experiments

- $\leq 0.03^{o}$ C discrepancies.
- FEA tilt ~20% less than from experiments.

→ **Ordinally sufficient for design iteration; discrepancies from:**

  - Uniform h loss.
  - Square contact modeling of couplings.
  - FEA is steady-state only.

Level (1 = bottom)	ΔT Segmented – Simulated	ΔT Segmented – Measured	ΔT One-Piece – Simulated	ΔT One-Piece – Measured
1	0.01	0.00 ± 0.01	0.07	0.06 ± 0.01
2	0.12	0.13 ± 0.02	0.12	0.09 ± 0.02
3	0.18	0.21 ± 0.03	0.12	0.12 ± 0.01
4	0.12	0.12 ± 0.02	0.12	0.09 ± 0.02
5	0.01	0.00 ± 0.01	0.07	0.06 ± 0.01

Source Placement

Sources aligned between couplings:
Thermal strain relief in the gaps.

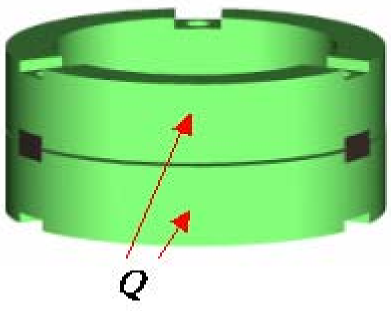

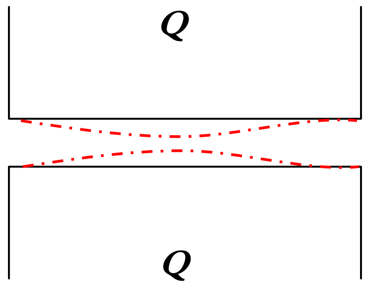

Sources aligned along couplings:
Thermal strain transmission across the gaps.

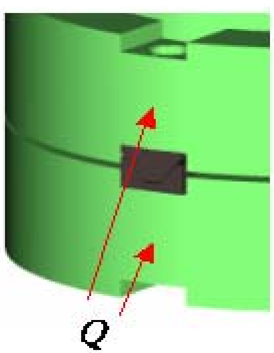

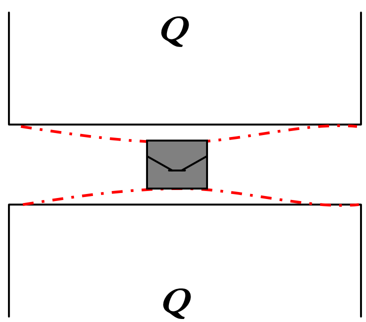

<u>**Comparison (FEA):**</u>

	Tilt – point-to-point	**Tilt – variance**
Segmented – Q between couplings	0.46	0.026
Segmented – Q along couplings	0.58	0.027
One-piece	0.70	0.034

Material Study

Material	Tilt – (Normalized)
Aluminum (6061-T651)	1.00
Copper	**0.35**
Brass	1.40
Stainless (AISI 1040)	4.20

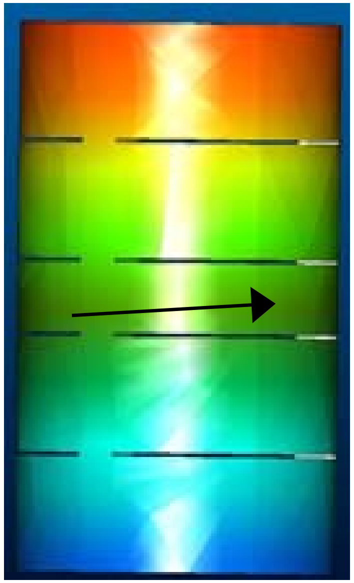

Copper

0.16 arcsec

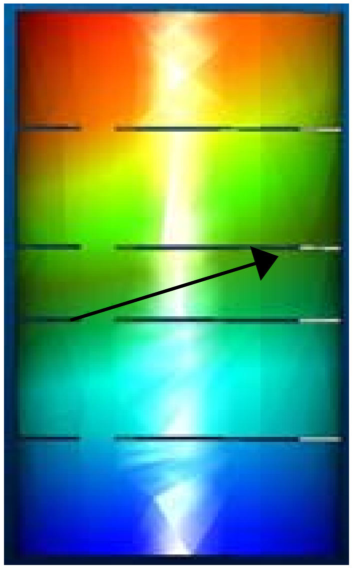

Stainless

1.93 arcsec

Copper vs. Stainless = 92% improvement

Copper vs. Aluminum = 72% improvement

Dimensional Analysis

Geometry of segmented structure – material properties fixed:

1. Dimensionless temperature difference across single segment:

$$\frac{(\Delta T)kD}{Q} = f\left(\frac{h}{t}\right)$$

2. Error motion of the stack:

$$\theta_{tilt} = f\left(\frac{h}{t}, \frac{h}{H}\right)$$

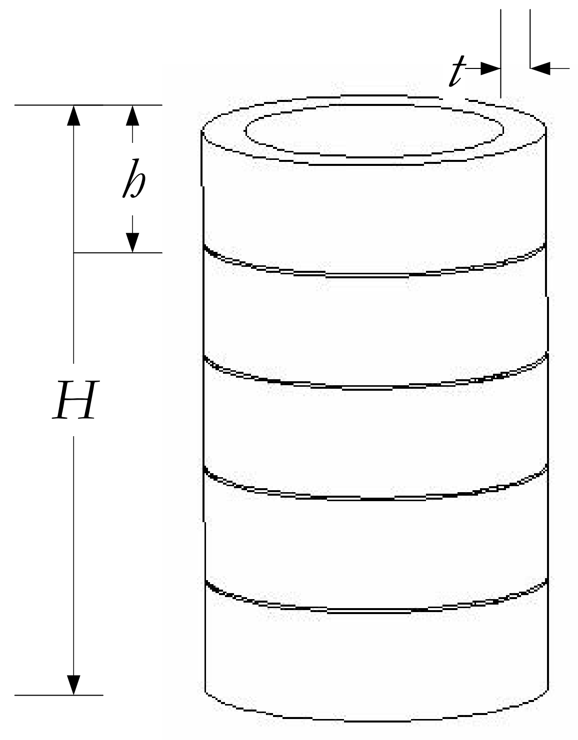

Geometry Optimization

Vary segment height (*h*) and segment thickness (*t*):

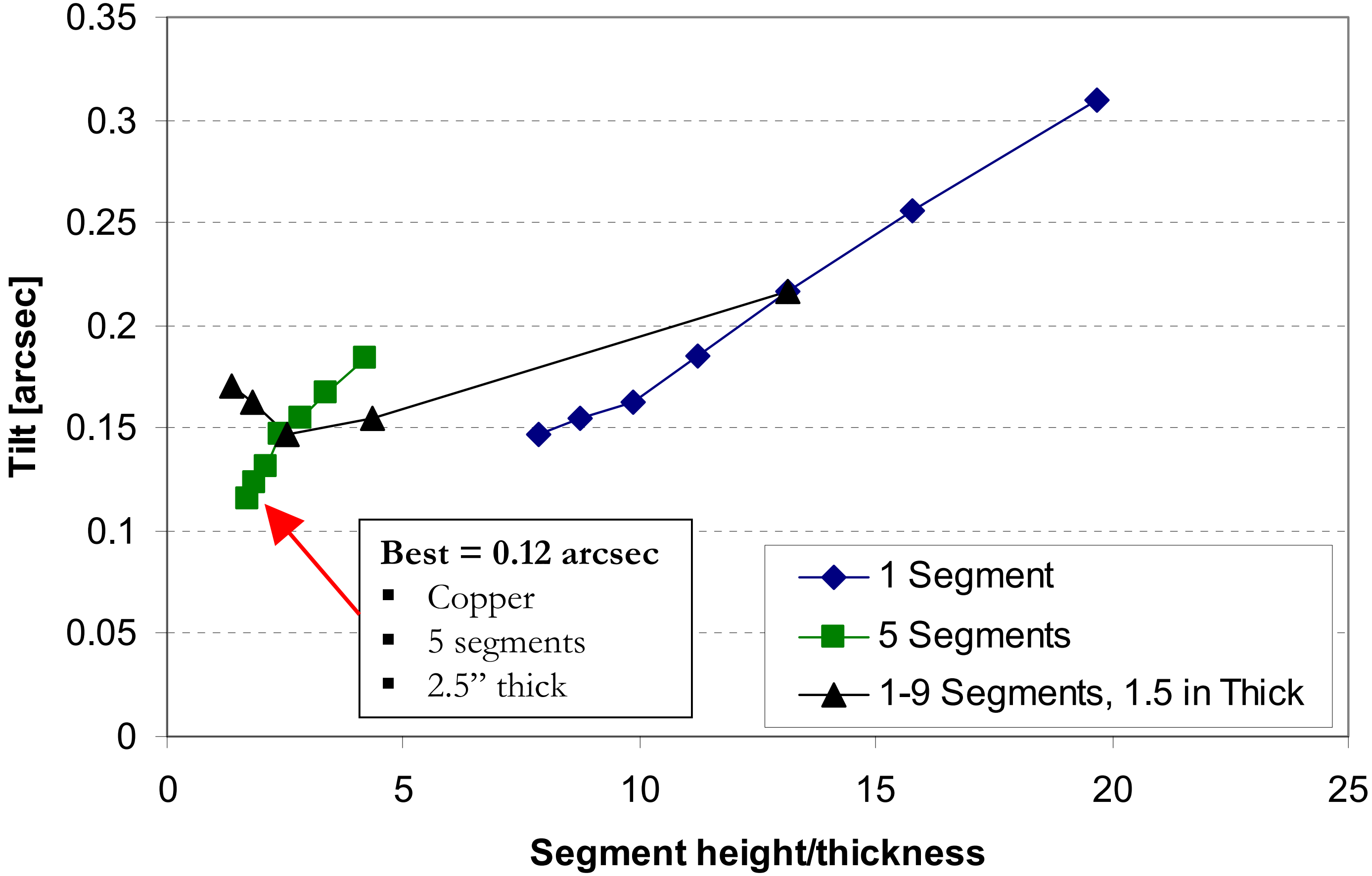

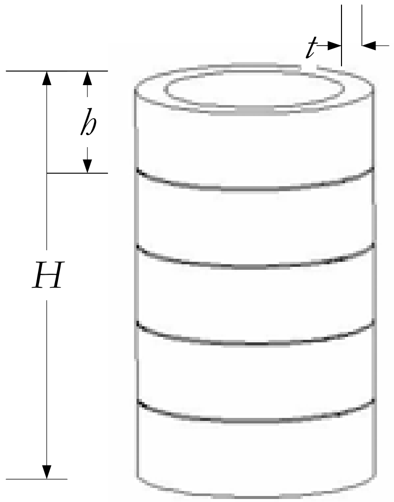

Thermal Shielding

Isolate tubes using concentric outer rings of insulation and high conductivity shielding:

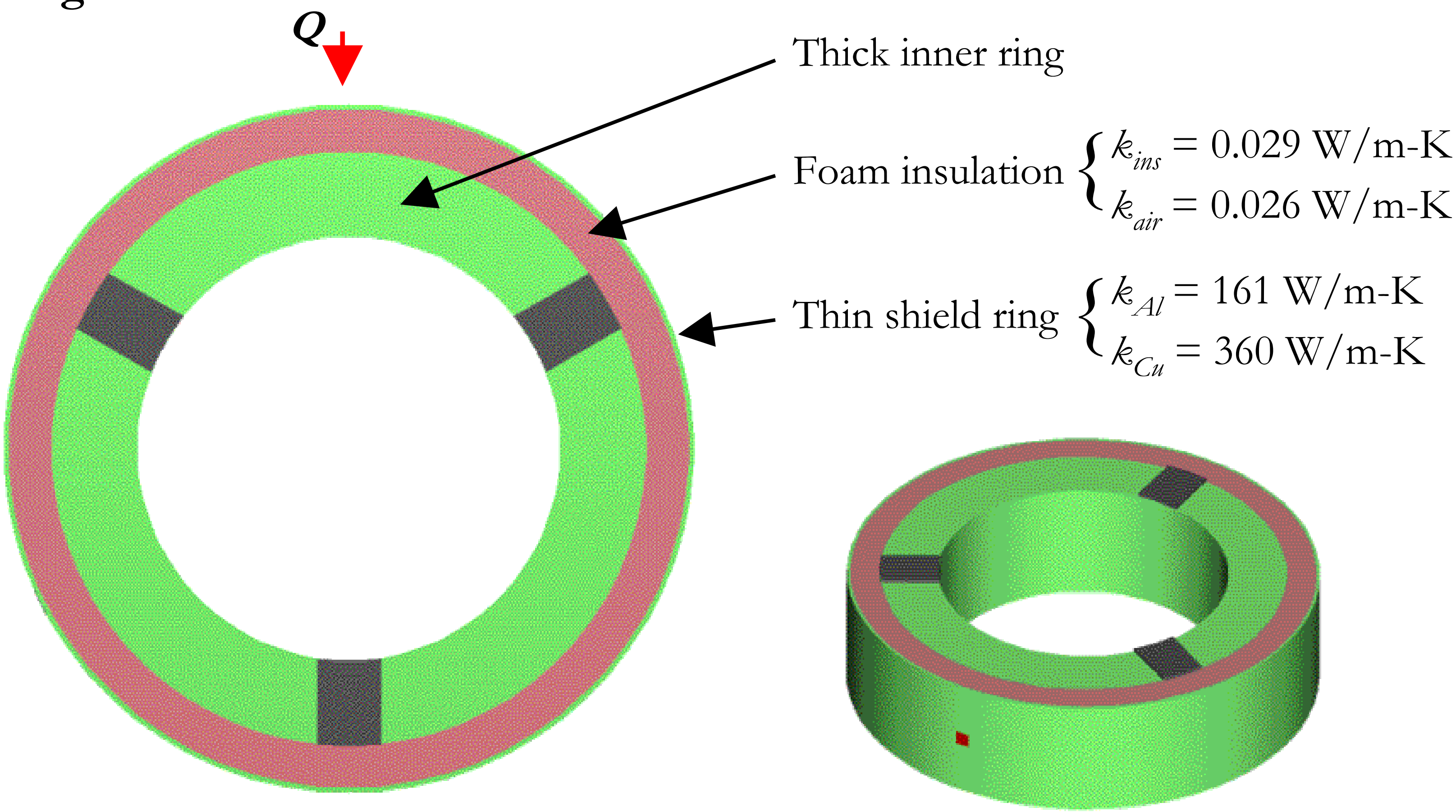

Shielding – FEA Results

Effect of shielding on tilt of a single segment: (Al inner only normalized to 1.00)

Design	**Tilt** [arcsec]: **No Insulation**	**Tilt** [arcsec]: **½" Insulation**	**Tilt** [arcsec]: **1" Insulation**
2" Al inner only	1.00	-	-
2" Cu inner only	**0.49**	-	-
2" Cu inner w/ no shield	-	0.36	**0.27**
2" Al inner w/ ⅛ " Al shield	-	0.38	0.33
2" Al inner w/ ⅛" Cu shield	-	0.35	0.27
2" Cu inner w/ ⅛" Cu shield	-	0.22	0.16
2" Cu inner w/ 1/16" Cu shield	-	0.19	**0.13**

Shielding – FEA Results

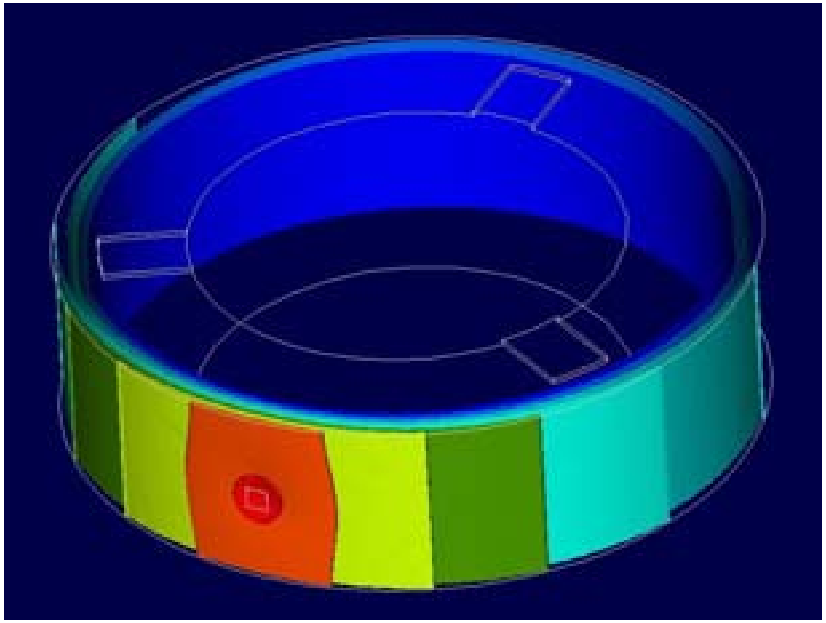

Temperature

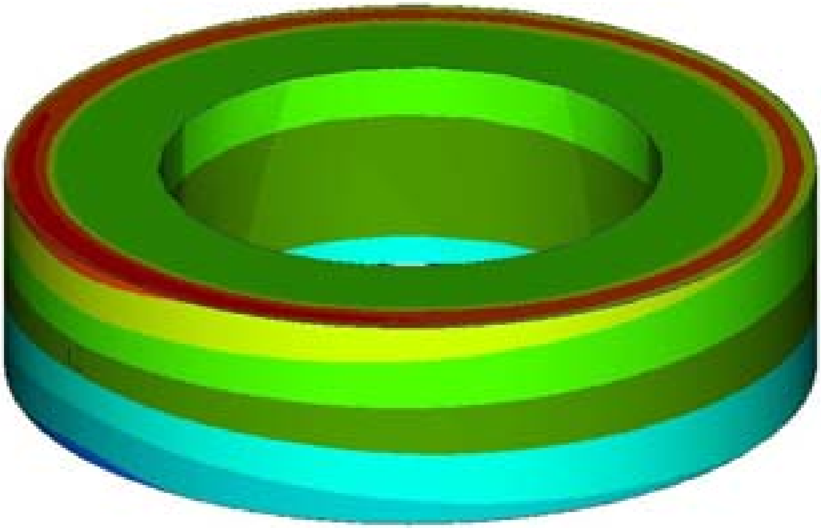

Displacement

Performance Trend

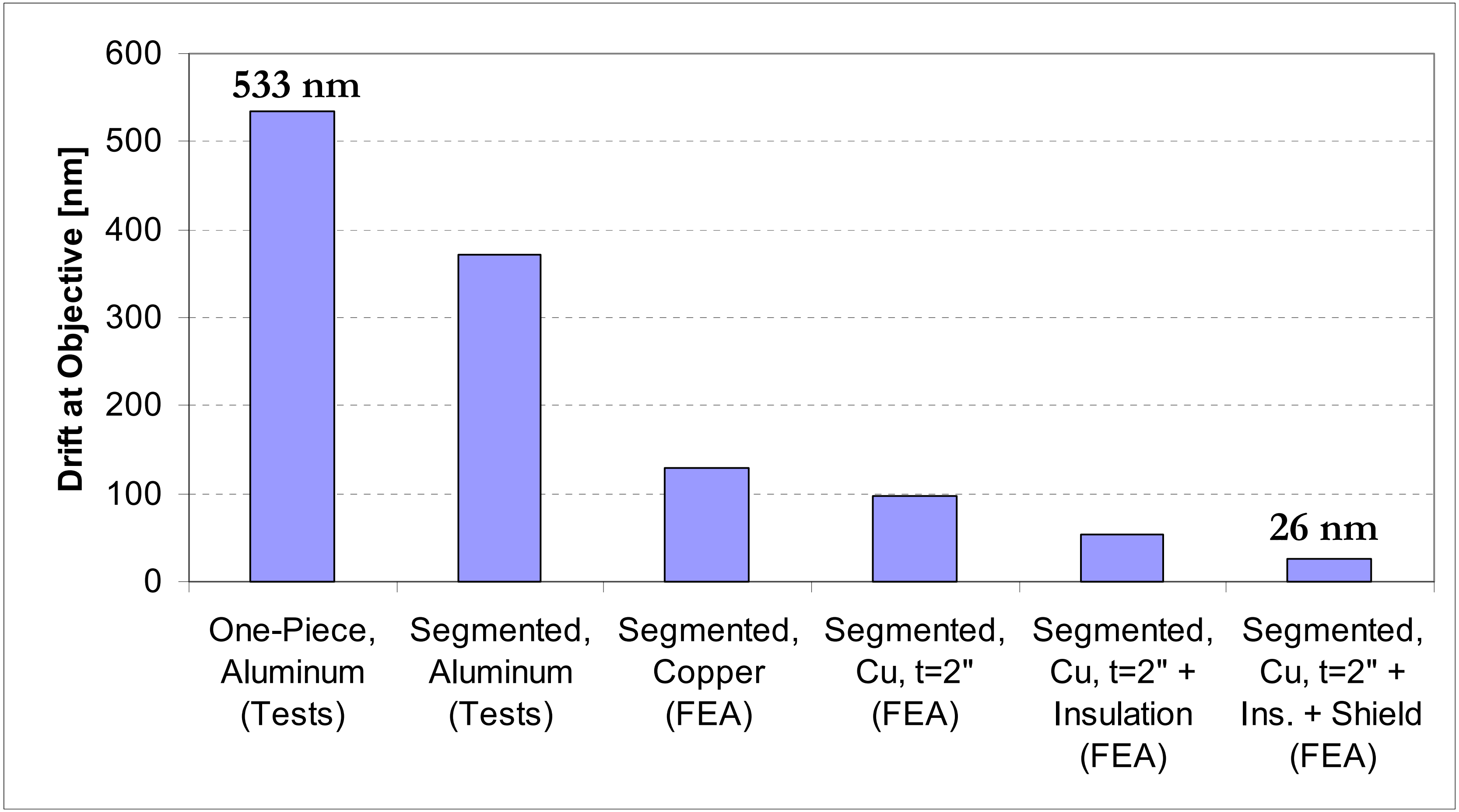

Cost vs. Performance

Cost of segmentation + shielding, versus:

- Solid, shielded Al or Cu structure?
- Solid Invar structure (rolled plate)?
- Segmented Invar structure?

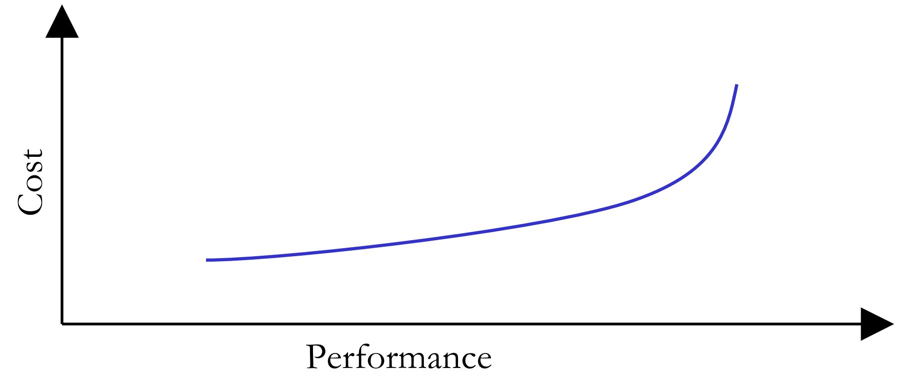

Tradeoffs:

- Functionality of segmentation vs. cost of couplings.
- Secondary machining costs for mounting for optics and stages.

<u>Invar?</u>

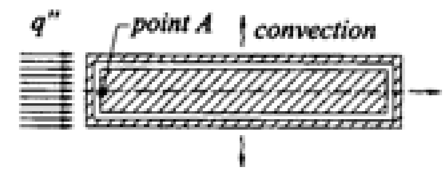

Configuration	*Frame deformation due to temperature gradients [nm]*		
	x-axis	*y-axis*	*z-axis*
Aluminium frame <u>with</u> shielding	5	5	15
Aluminium frame <u>without</u> shielding	100	100	300
Invar frame <u>with</u> shielding	2	2	7
Invar frame <u>without</u> shielding	45	45	135

*Ruiji, Theo. Ultra Precision Coordinate Measuring Machine, Ph.D. Thesis, Eindhoven, The Netherlands, 2001, p.66.

Implications

Segmenting improves dynamic thermal accuracy and interchangeability:

- Segmentation reduces tilt error:
  - 57% transient.
  - 31% near-steady-state.
- Thin sheet shielding and/or insulation reduces additional 3x-6x.
- Best case simulated = 144 nm at objective under 3x1W localized sources.
- Kinematic couplings give high gap resistance and enable precision modularity.

Next Steps:

- Improve transient analytical model.
- Transient design study and comparison to steady-state results.
- Study sensitivity to magnitude, intensity, and location of sources.
- Design, testing, and packaging of flexure mounts.

References

1. "Overview of the High Precision Microscope Project", University of Illinois Laboratory for Fluorescence Dynamics, 2000.
2. Hetnarski, Richard (ed.). Thermal Stresses, New York, NY: North-Holland, 1986.
3. Leinhard, John IV, and John Leinhard V. A Heat Transfer Textbook, Cambridge, MA: Phlogiston Press, 2001.
4. Ho, Y.C. "Engineering Sciences 205 Class Notes", Harvard University, 2001.
5. Slocum, Alexander H. and Alkan Donmez. "Kinematic Couplings for Precision Fixturing - Part 2: Experimental Determination of Repeatability and Stiffness", Precision Engineering, 10.3, July 1988.
6. Mullenheld, Bernard. "Prinzips der kinematischen Kopplung als Schnittstelle zwischen Spindel und Schleifscheibe mit praktischer Erprobung im Vergleich zum Kegel-Hohlschaft" (Transl: Application of kinematic couplings to a grinding wheel interface), SM Thesis, Aachen, Germany, 1999.
7. Araque, Carlos, C. Kelly Harper, and Patrick Petri. "Low Cost Kinematic Couplings", MIT 2.75 Fall 2001 Project, http://psdam.mit.edu/kc.
8. Hart, John. "Design and Analysis of Kinematic Couplings for Modular Machine and Instrumentation Structures", SM Thesis, Massachusetts Institute of Technology, 2001.
9. Slocum, Alexander. Precision Machine Design, Dearborn, MI: Society of Manufacturing Engineers, 1992.
10. Ruiji, Theo. Ultra Precision Coordinate Measuring Machine, Ph.D. Thesis, Eindhoven, The Netherlands, 2001.

Acknowledgements

- Prof. Alex Slocum, Advisor
- Matt Sweetland – Collaboration on tube and coupling prototype design.
- Philip Loiselle – Assistance in measurement setup and data acquisition.

Central Column – Normalized Temp

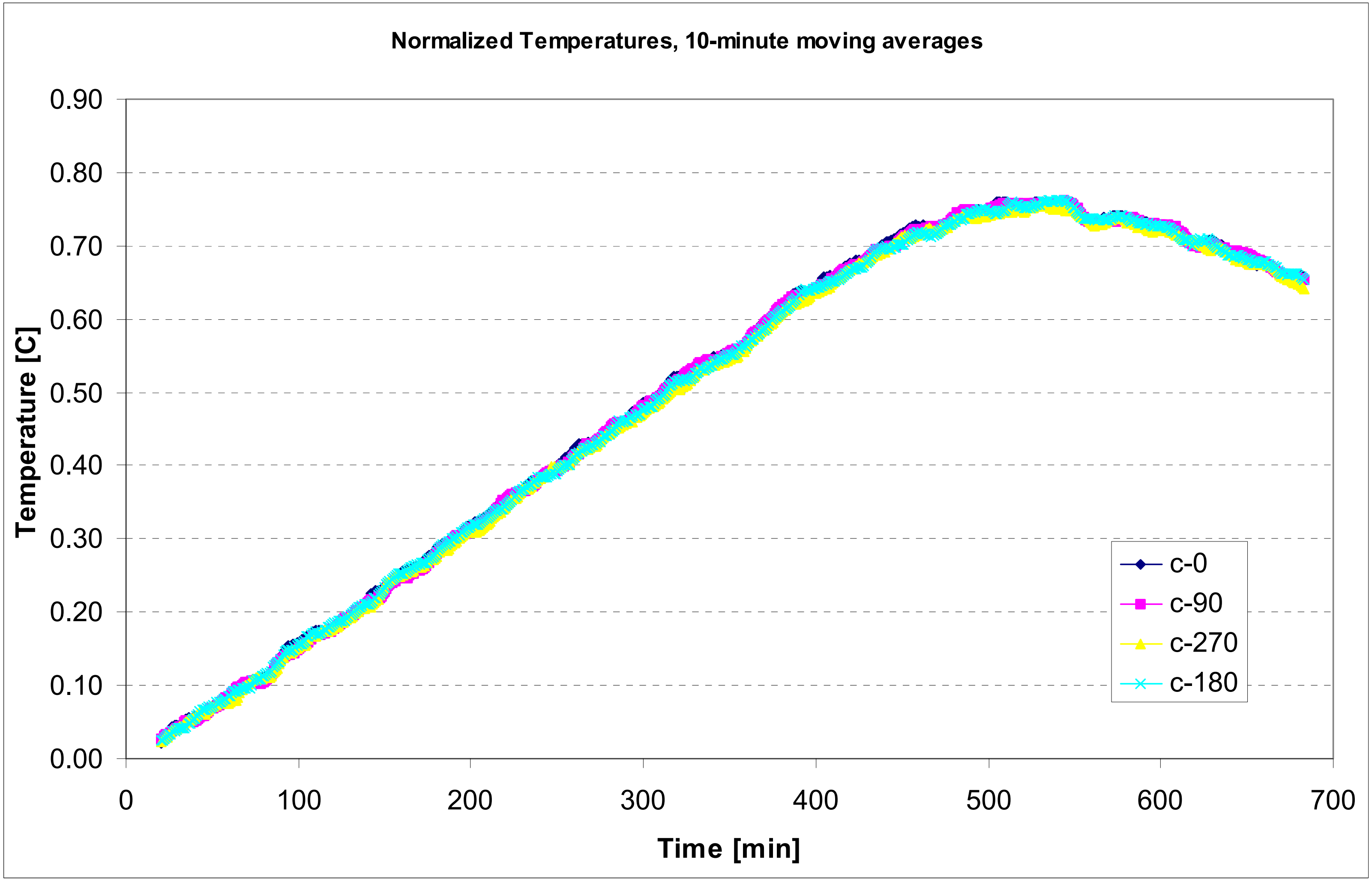

Central Column – Temp Range

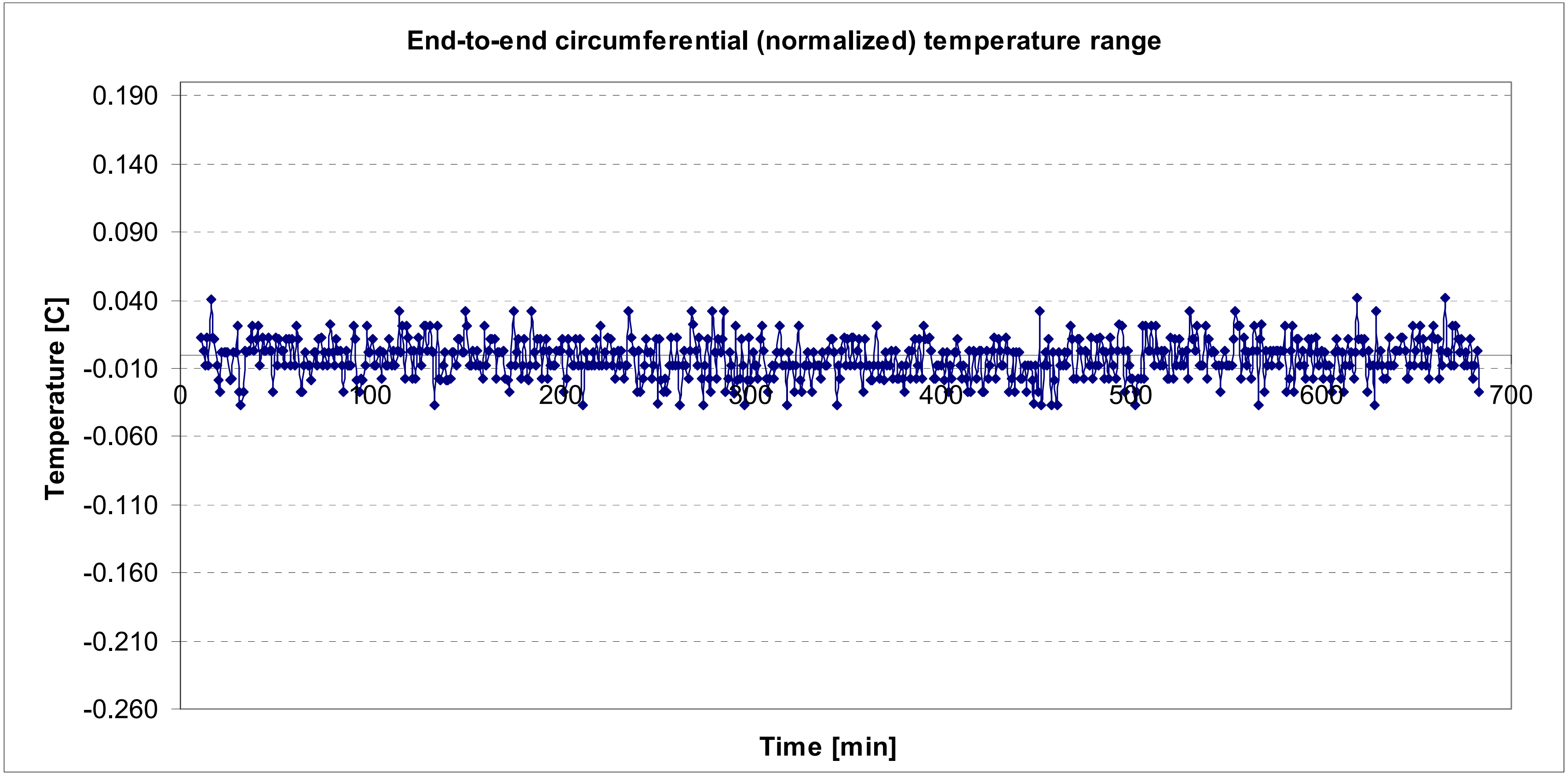

Central Column – Temp Range

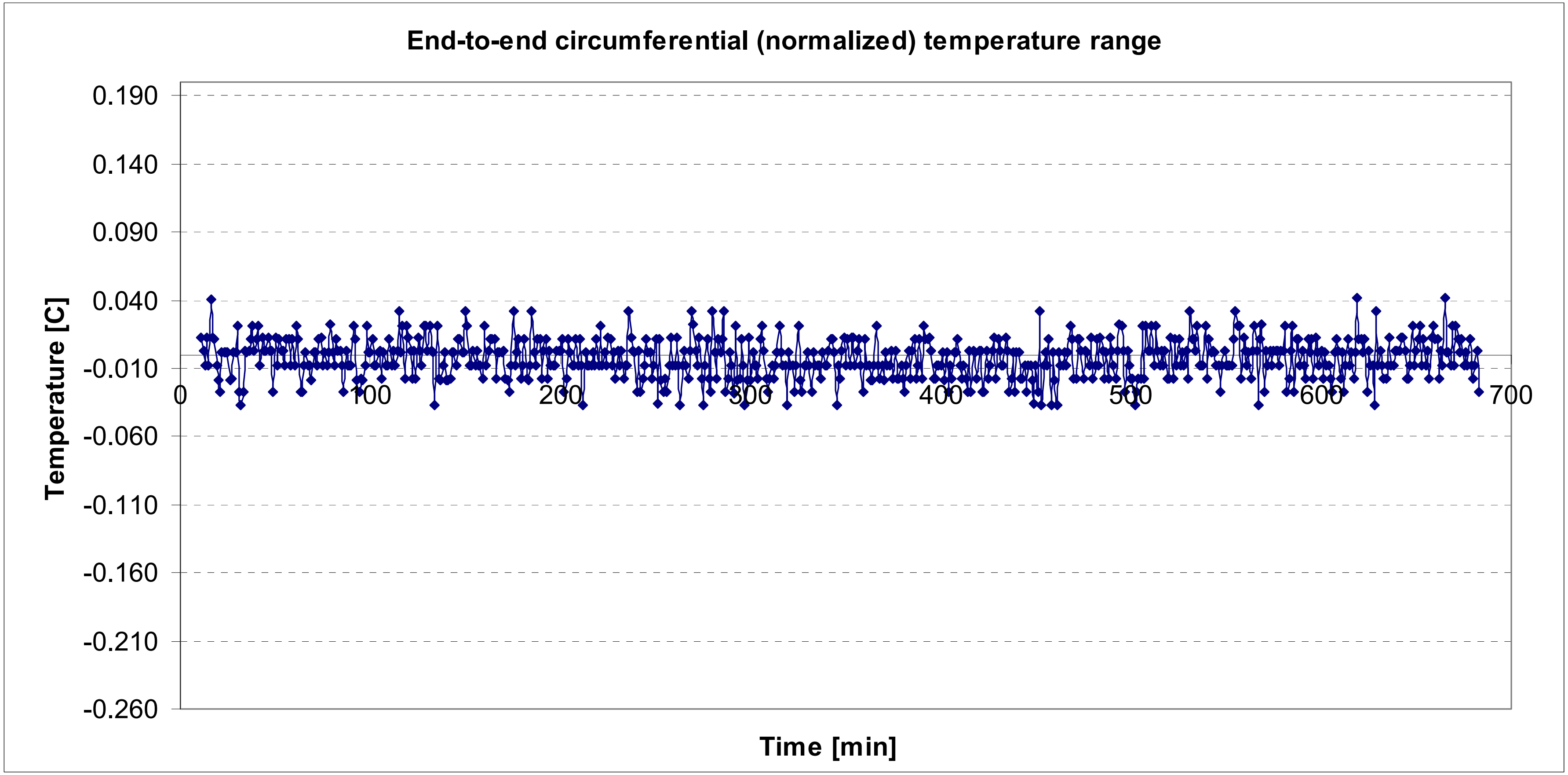

One-Piece – Central Level Response

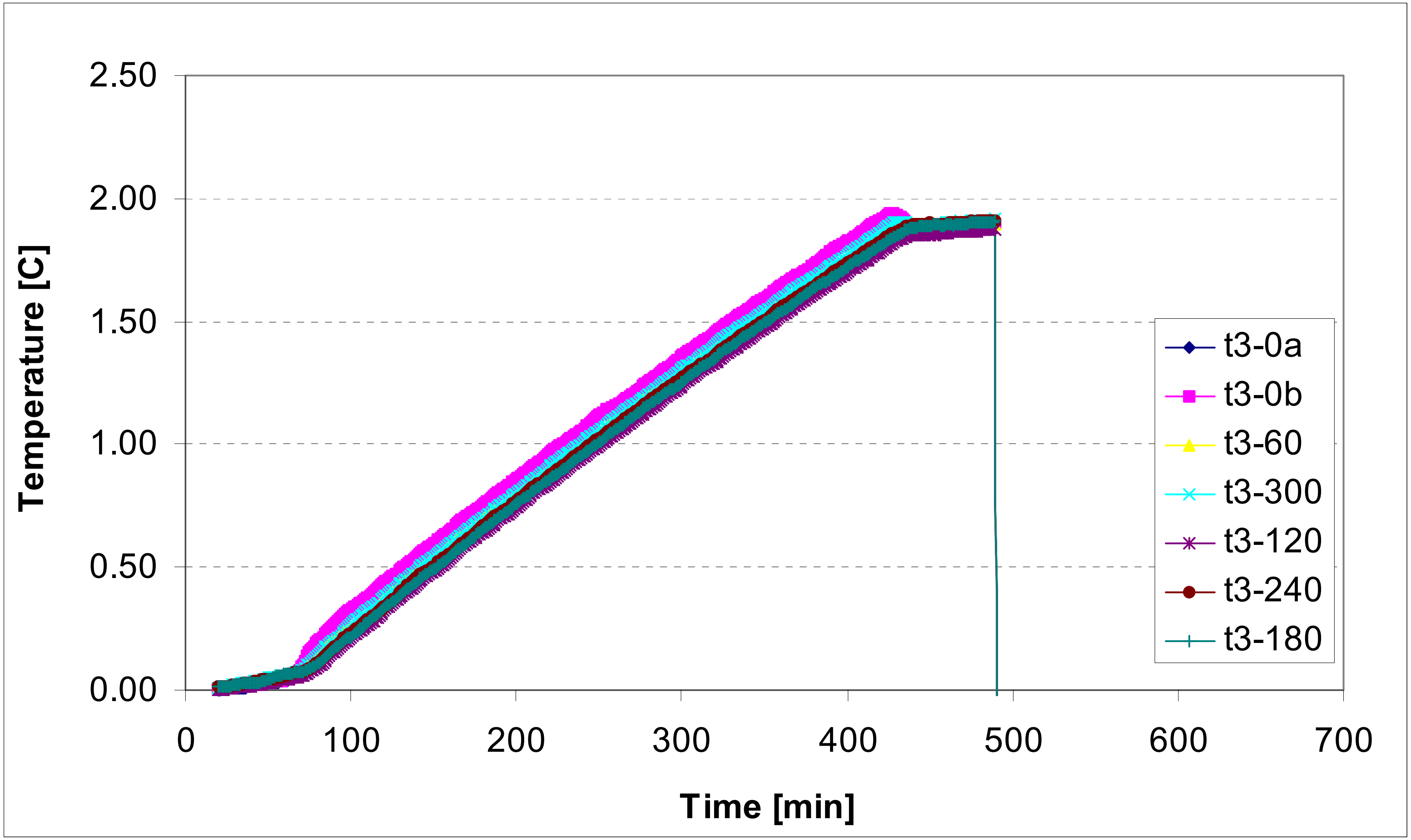

Room Temperature

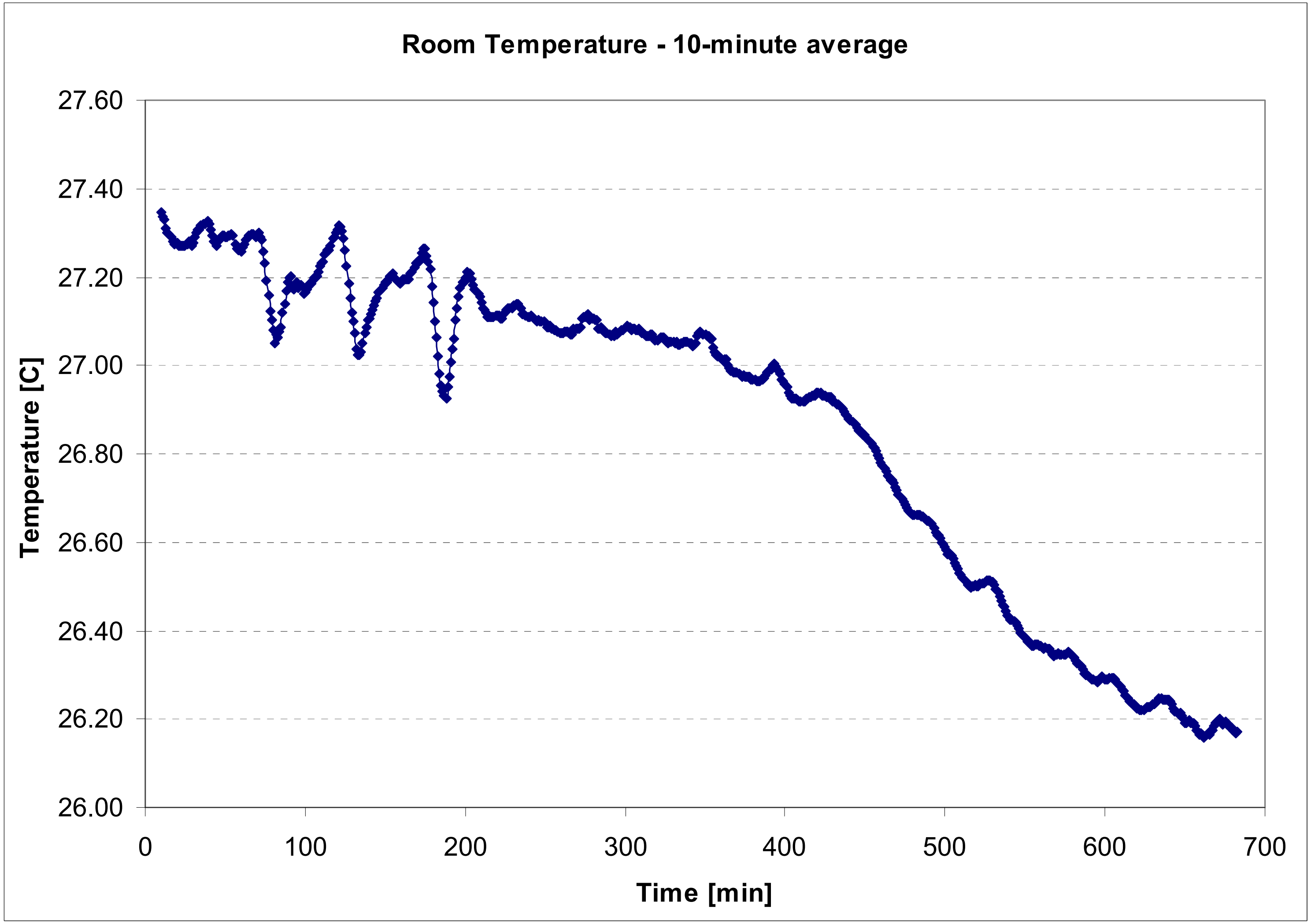

Shielding – Transient Performance

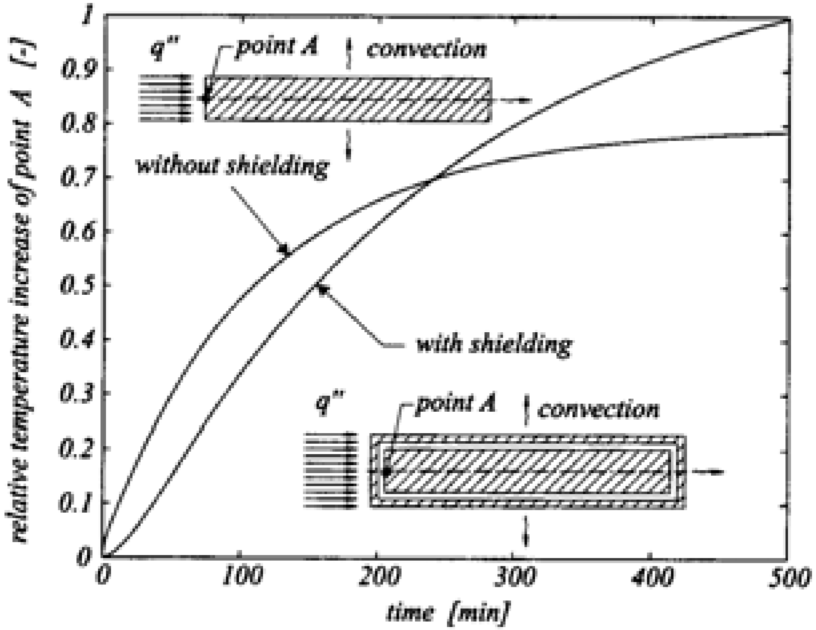

FIGURE 3.14: Temperature increase of point A on the left face of the aluminium frame due to a heat flux q'', with or without the aluminium thermal shielding. Note that the temperature increase after 500 minutes of the aluminium frame with thermal shielding is scaled to unity.

*Ruiji, Theo. Ultra Precision Coordinate Measuring Machine, Ph.D. Thesis, Eindhoven, The Netherlands, 2001, p.68.

Shielding – Transient Performance

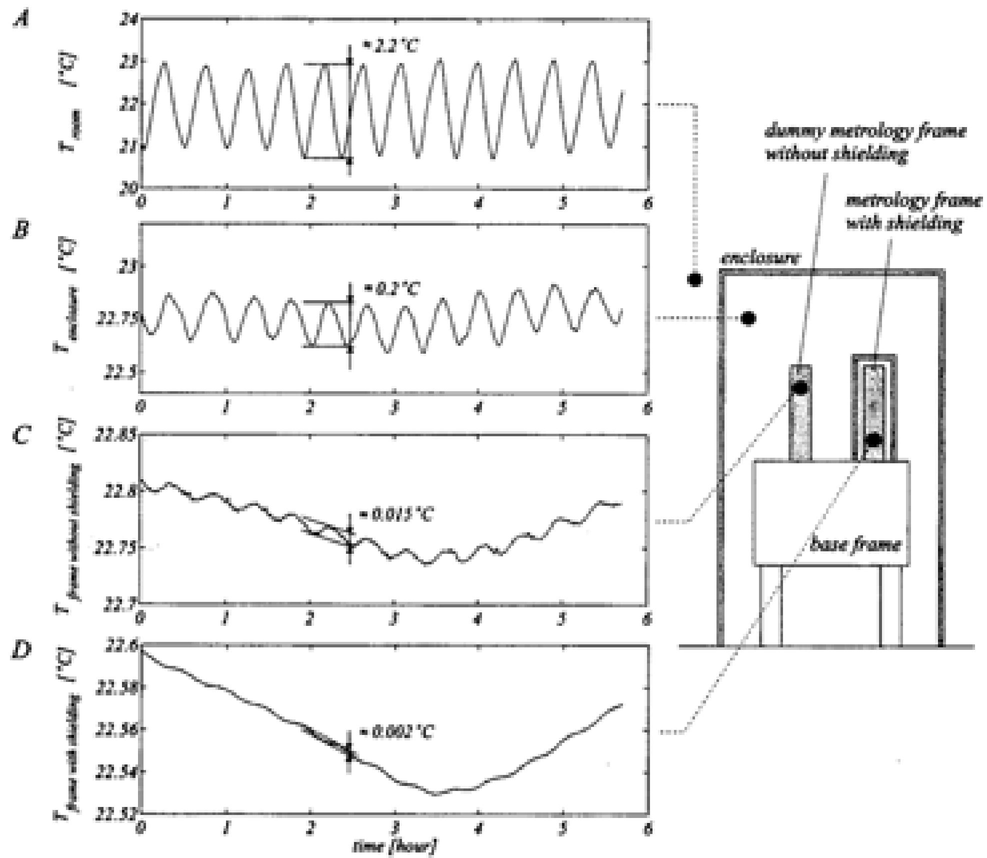

FIGURE 7.14: Reductions of the fast temperature variations (cycle time 30 minutes) due to the thermal insulation by the enclosure and the thermal shielding.

*Ruiji, Theo. Ultra Precision Coordinate Measuring Machine, Ph.D. Thesis, Eindhoven, The Netherlands, 2001, p.165.

Shielding – Transient Performance

Configuration	Frame deformation due to temperature gradients [nm]			Frame expansion due to uniform temperature increase [nm]		
	x-axis	y-axis	z-axis	x-axis	y-axis	z-axis
Aluminium frame with shielding	5	5	15	420	520	960
Aluminium frame without shielding	100	100	300	420	520	960
Invar frame with shielding	2	2	7	15	18	33
Invar frame without shielding	45	45	135	15	18	33

TABLE 3.2: Thermal bending deformations and linear expansions of the metrology frame along the x, y and z-axis due to thermal gradients and increase of the average frame temperature.

*Ruiji, Theo. Ultra Precision Coordinate Measuring Machine, Ph.D. Thesis, Eindhoven, The Netherlands, 2001, p.66.

Kinematic Coupling Interfaces

Designed “canoe ball” kinematic couplings as segment interconnects:

- CNC cylindrical ground from 420 Stainless Steel (RC ~55) with 250 mm radius spherical contact surfaces.
- Stiffness gain: $G_s = \left(\frac{R_{canoe}}{R_{traditional}} \right)^{\frac{1}{3}}$
- Load capacity gain: $G_l = \left(\frac{R_{canoe}}{R_{traditional}} \right)^{2}$
- Documented repeatability gain:
  Traditional ball-groove = 500 nm [5]
  Canoe ball = 100 nm [6]
  Coated canoe ball = 54 nm [7]
- Equal 120^{o} angle arrangement maximizes uniformity of radial expansion.

Repeatability vs. Interchangeability

Kinematic couplings are known for excellent repeatability, yet interchangeability is limited by manufacturing and placement errors for the balls and grooves [8]:

Repeatability - The tendency of the centroidal frame of the top half of the interface to return to the same position and orientation relative to the centroidal frame of the fixed bottom half when repeatedly detached and re-attached.

Interchangeability - The tendency of the centroidal frame of the top half of the interface to return to the same position and orientation relative to the centroidal frames of different fixed bottom halves when switched between them.

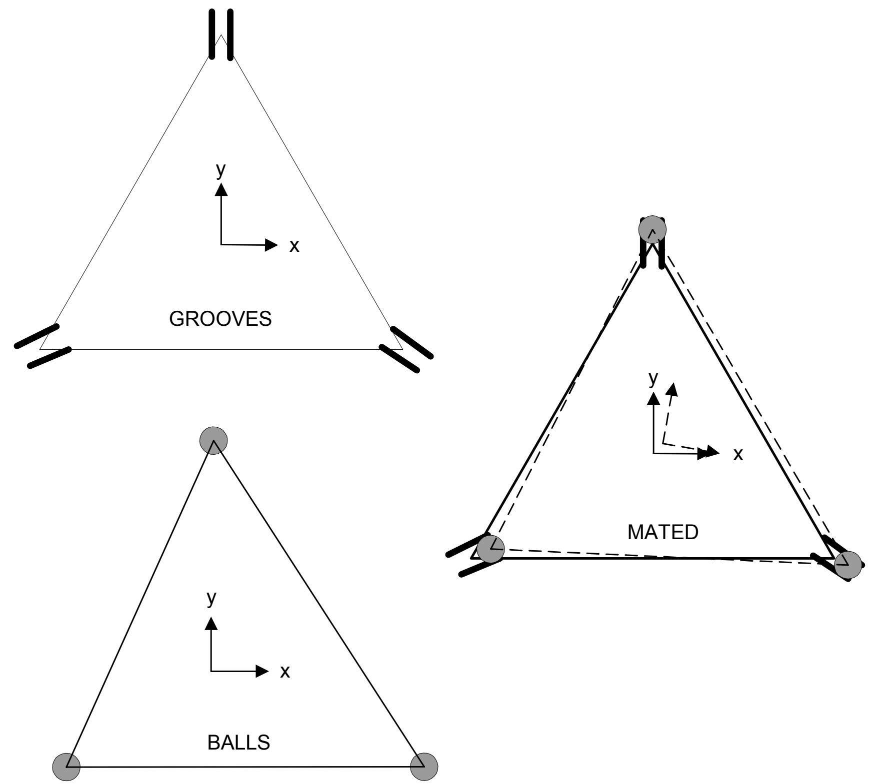

Interchangeability Model

Calculate and correct for interchangeability error caused by coupling variation:

1. Use a CMM to measure the locations and sizes of contact surfaces on balls and grooves.
2. Assuming deterministic mating, calculate the error introduced by the measurement deviations from nominal.
3. Express this error as a homogeneous transformation matrix (HTM), and add it to the serial kinematics of the structure:

$$T_{error-Full} = \left(T_{Ball-TCP}\right)^{-1} T_{Groove-Work} \qquad T_{error-Resid} = \left(T_{interface} T_{Ball-TCP}\right)^{-1} T_{Groove-Work}$$

GOALS:

1. Measure an individual coupling and reduce the error at a point of interest by calculating and correcting for $T_{interface}$.
2. Knowing distribution parameters of a manufacturing process, predict the interchangeability error of a large population.
3. Predict the interchangeability error of a large population as a function of manufacturing tolerances and calibration detail, enabling accuracy / best cost choices.

Interchangeability Error Model

Consider stackup of errors in coupling manufacturing, mounting plate manufacturing, and coupling-to-plate assembly:

For example in z-direction of a ball mount, tolerances:

- Sphere radius = δ_{Rsph}
- Contact point to bottom plane = δ_{hR}
- Measurement feature height = δ_{hmeas}
- Protrusion height = δ_{hprot}

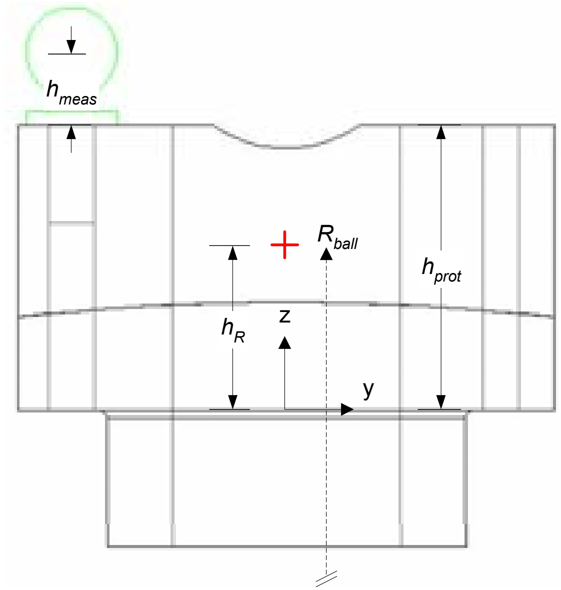

$$\varepsilon_z = \frac{1}{2}\left(\left(\frac{2\left(\frac{\delta_{Rsph}}{\sqrt{2}}\right)+\delta_{hR}+\delta_{hprot}+\delta_{hmeas}+}{\sqrt{2\left(\frac{\delta_{Rsph}}{\sqrt{2}}\right)^2+\delta_{hR}{}^2+\delta_{hprot}{}^2+\delta_{hmeas}{}^2}}\right)\right)$$

Each dimension is perturbed by generating a random variate, e.g. for mounting hole placement:

$$x_{h_{b_1}} = x_{h_{b_1 nom}} + \delta_{R,h_{b_1}}\delta_{pos}\mathrm{RandN}()\cos(\theta_{rand})$$

$$y_{h_{b_1}} = y_{h_{b_1 nom}} + \delta_{R,h_{b_1}}\delta_{pos}\mathrm{RandN}()\sin(\theta_{rand})$$

$$\theta_{rand} = 2\pi\mathrm{Rand}()$$

Interface Error Model – Block Diagram

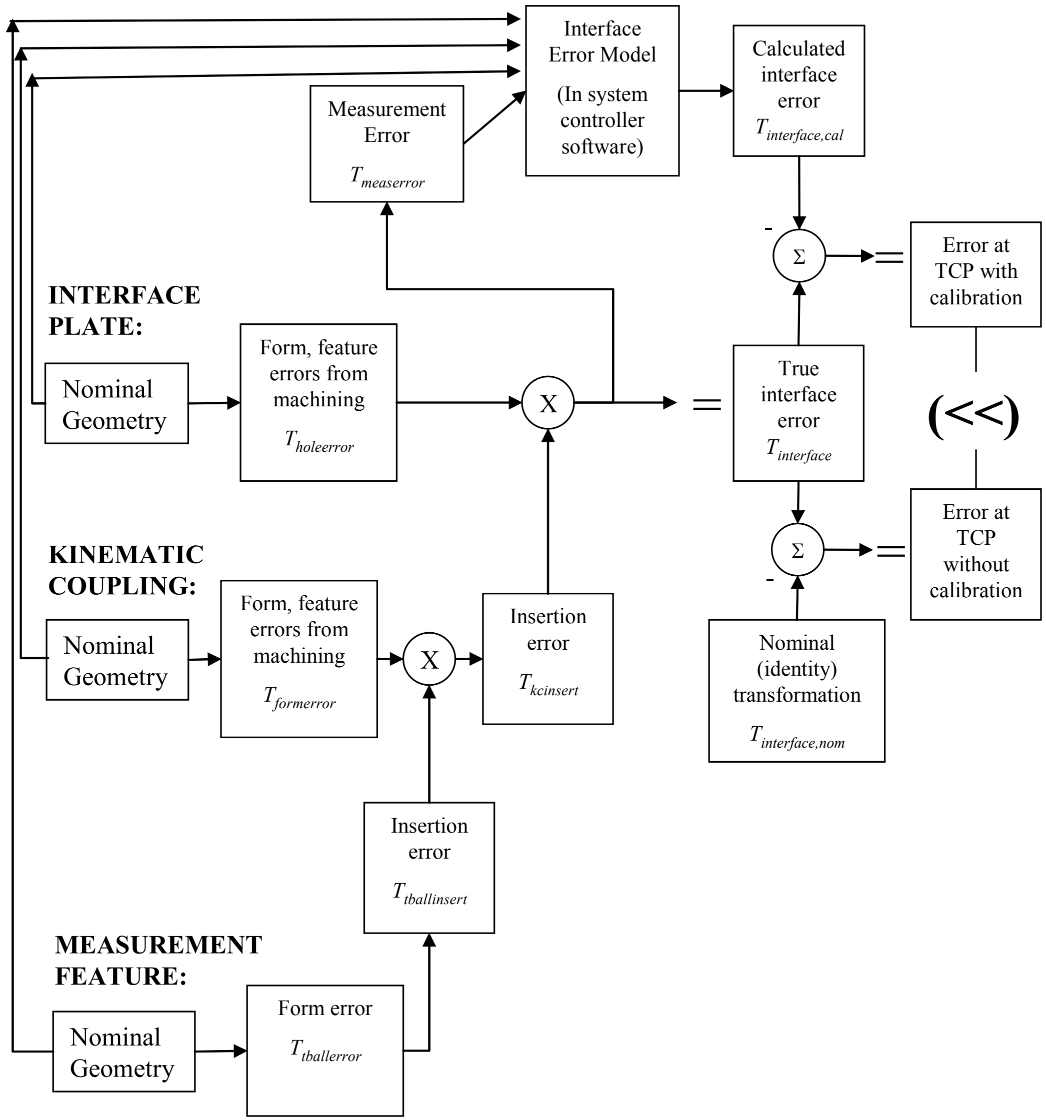

Interchangeability Solution Method

Linear system of 24 constraint equations between the balls and grooves – accounts for both positional and angular misalignment:

1. Contact sphere centers must be at minimum (normal) distance between the groove flats, e.g.:

$$\frac{(q_1 - b_1)\cdot N_1}{\|N_1\|} = R_1$$

q_1, b_1 = initial, final center positions;
N_1 = groove normal; R_1 = sphere radius.

2. By geometry, the combined error motion of contact spheres is known with respect to the error motion of their mounting plate. For small angles, e.g.:

$$\begin{aligned}
\mathrm{x}_{s,1} &= \delta_{x_c} + \mathrm{u}_{s,1} + \mathrm{v}_{s,1}\left[-\theta_{z_c}\right] + \mathrm{w}_{s,1}\left[\theta_{y_c}\right]\\
\mathrm{y}_{s,1} &= \delta_{y_c} + \mathrm{u}_{s,1}\left[\theta_{z_c}\right] + \mathrm{v}_{s,1} + \mathrm{w}_{s,1}\left[-\theta_{x_c}\right]\\
\mathrm{z}_{s,1} &= \delta_{z_c} + \mathrm{u}_{s,1}\left[-\theta_{y_c}\right] + \mathrm{v}_{s,1}\left[\theta_{x_c}\right] + \mathrm{w}_{s,1}
\end{aligned}$$

$(q_{S,1}, q_{S,1}, q_{S,1})$ = initial center positions;
$(x_{S,1}, y_{S,1}, z_{S,1})$ = final center positions.

3. Solve linear system and place six error parameters in HTM:

$$T_{interface} = \begin{bmatrix} 1 & -\theta_{z_c} & \theta_{y_c} & \delta_{x_c} \\ \theta_{z_c} & 1 & -\theta_{x_c} & \delta_{y_c} \\ -\theta_{y_c} & \theta_{x_c} & 1 & \delta_{z_c} \\ 0 & 0 & 0 & 1 \end{bmatrix}$$

Monte Carlo Simulation Tool

MATLAB routine for calculating interface interchangeability:

<u>Variable input parameters:</u>

- Number of iterations
- Calibration complexity
- Magnitude of individual tolerances.

<u>For each iteration:</u>

- Generates random variates and adds them to nominal dimensions.
- Determines mating position of interface with perturbed dimensions.
- Calculates perfect interface transformation.

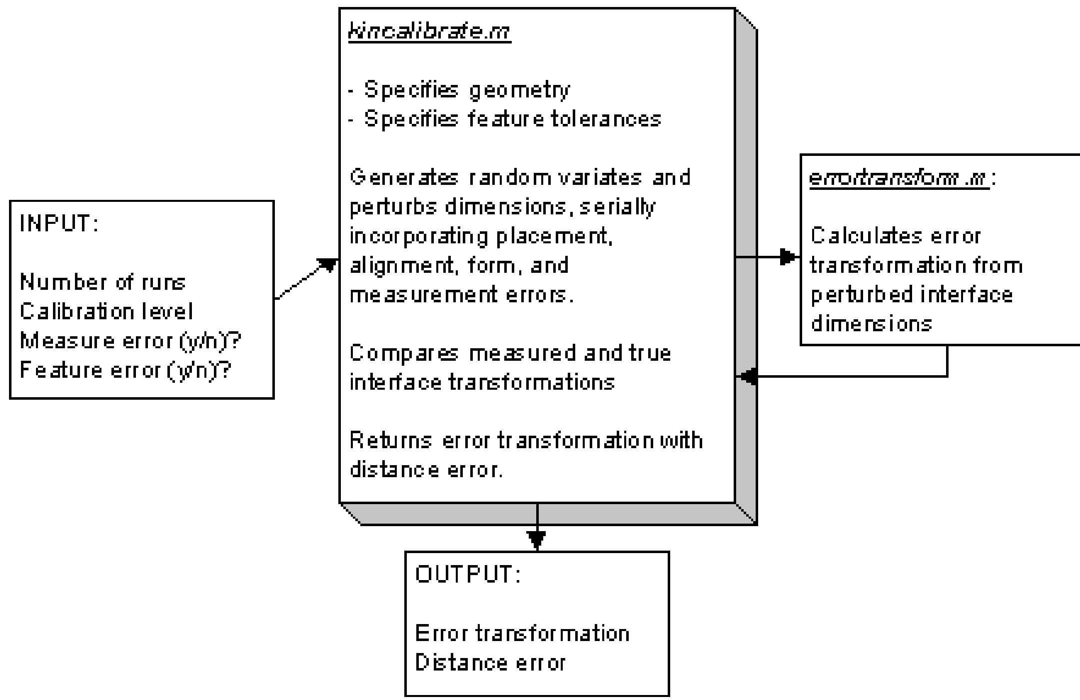

Simulation Results – Industrial Process

Simulations, varying the complexity of calibration:

- Level 0 = no measurement; Level max = measurement of all contacts.
- Offset feature is a tooling ball or hemisphere on the coupling mount, use nominal offsets to estimate contact points.
- Direct measurement simulates CMM measurement of contact spheres and groove flats.

Using offset measurement feature:

- 0.11 mm interchangeability at full calibration

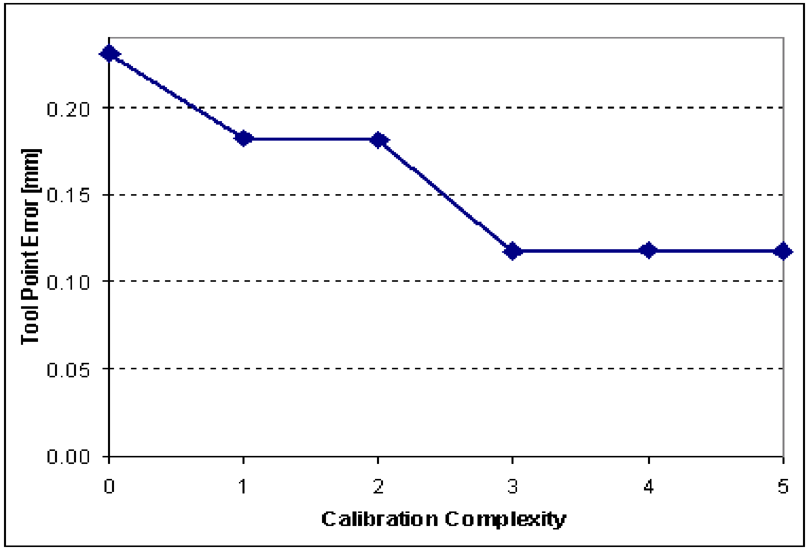

Using direct measurement:

- 0.02 mm interchangeability at full calibration

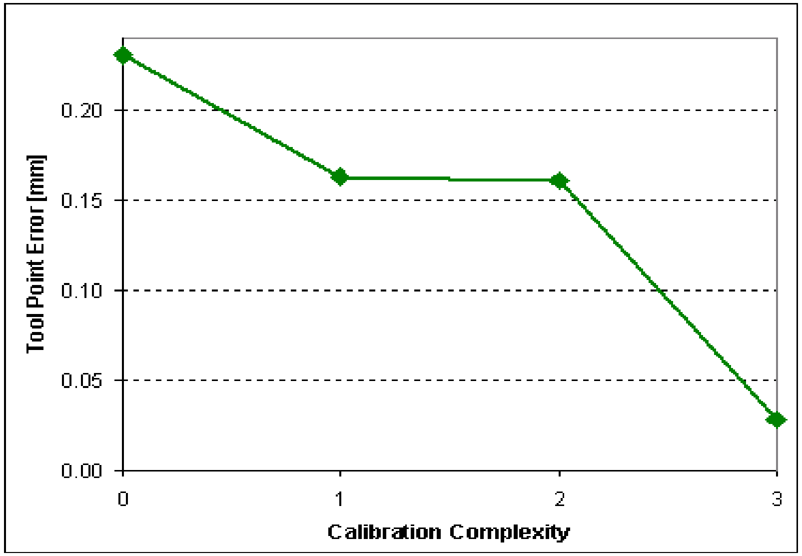

Model Validation

CMM measurements of 54 ball/groove pallet/base combinations:

1. Each piece CNC machined, with individual dimensional perturbations applied.
2. Average error before interface calibration = 1.5×10^{-3} rad.
3. Average error after interface calibration = 1.4×10^{-4} rad = **92% reduction**.

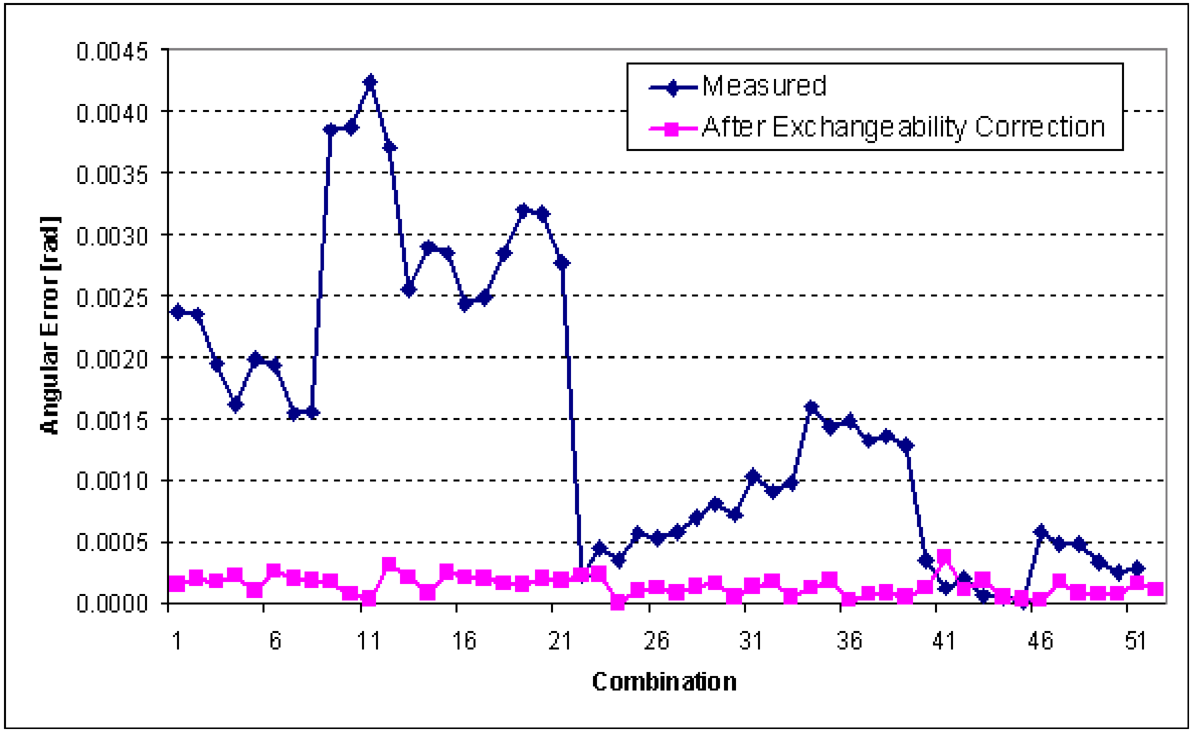

Application: Industrial Robots

Designed quick-change factory interface for ABB IRB6400R manipulator:

- A repeatable, rapidly exchangeable interface between the foot (three balls/contactors) and floor plate (three grooves/targets).

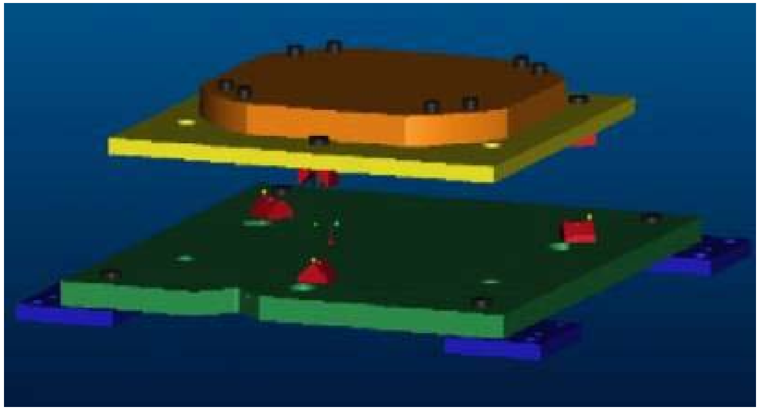

Installation Process:

- Calibrate robots at ABB to a master baseplate
- Install production baseplates at the customer site and calibrated the kinematic couplings directly to in-cell tooling.
- Install robot according to refined mounting process with gradual, patterned preload to mounting bolts.
- TCP-to-tooling relationship is a deterministic frame transformation.
- Base calibration data handling is merged with ABB software.

Application: Industrial Robots

Base "Quick-Change" Accuracy = Repeatability + Interchangeability

			(measured)		(simulated)
Canoe balls (offset):	0.18 mm	=	0.06	+	0.12
Canoe balls (direct):	0.09 mm	=	0.06	+	0.03
Three-pin (direct):	0.10 mm	=	0.07	+	0.03

- Direct measurement of coupling contacts gives design meeting error target.
- **Total Interface Accuracy** = Repeatability + Interchangeability, near-deterministic prediction of error in blind mounting from a large population.